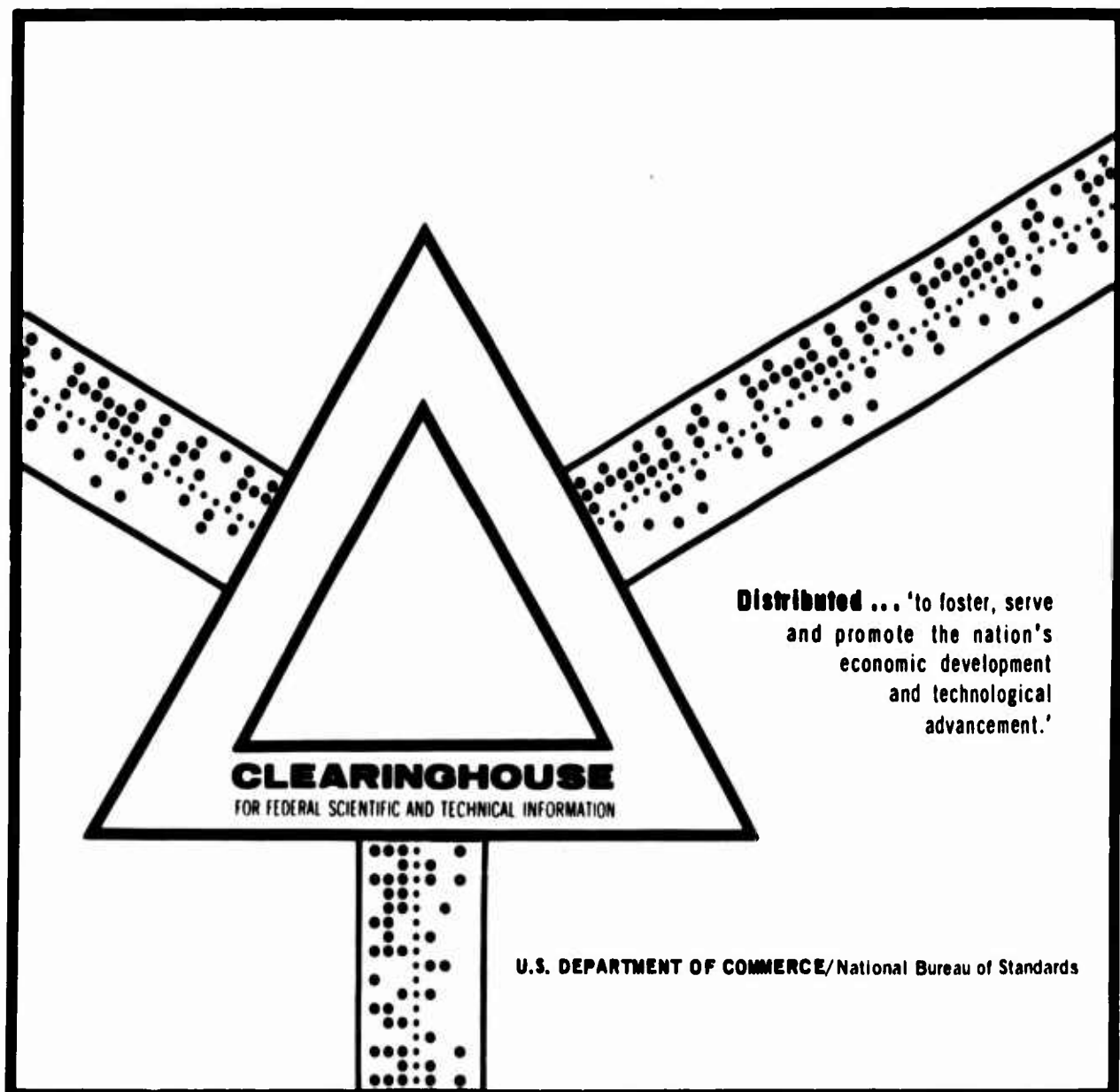AD 700 422

RESEARCH ON OCULAR LASER THRESHOLDS

Arthur Vassiliadis, et al

Stanford Research Institute
Menlo Park, California

August 1969

CLEARINGHOUSE
FOR FEDERAL SCIENTIFIC AND TECHNICAL INFORMATION

Distributed ... 'to foster, serve and promote the nation's economic development and technological advancement.'

U.S. DEPARTMENT OF COMMERCE/ National Bureau of Standards

This document has been approved for public release and sale.
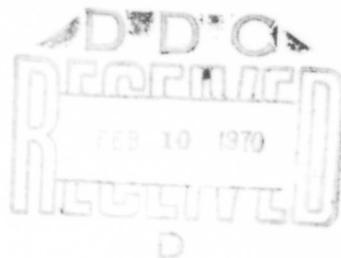
AD700422

Final Report

RESEARCH ON OCULAR LASER THRESHOLDS

By: A. VASSILIADIS   R. C. ROSAN   H. C. ZWENG

Prepared for:

UNITED STATES AIR FORCE
SCHOOL OF AEROSPACE MEDICINE
AEROSPACE MEDICAL DIVISION
BROOKS AIR FORCE BASE, TEXAS

D D C
RECEIVED
FEB 10 1970
D

STANFORD RESEARCH INSTITUTE
Menlo Park, California 94025 · U.S.A.

86

STANFORD RESEARCH INSTITUTE
Menlo Park, California 94025 · U.S.A.

RESEARCH ON OCULAR LASER THRESHOLDS

By: A. VASSILIADIS   R. C. ROSAN   H. C. ZWENG

Prepared for:

UNITED STATES AIR FORCE
SCHOOL OF AEROSPACE MEDICINE
AEROSPACE MEDICAL DIVISION
BROOKS AIR FORCE BASE, TEXAS

CONTRACT F41609-68-C-0041

SRI Project 7191

Approved:

R. C. HONEY, *Director*
Electromagnetic Techniques Laboratory

RAY L. LEADABRAND, *Executive Director*
Electronics and Radio Sciences Division

ABSTRACT

Results of experimental investigations of threshold levels for small retinal lesions are presented. Data for rhesus monkeys include threshold for a Q-switched neodymium laser, both in the macula and in the paramacular area. In addition, extensive data are presented for argon, helium-neon, and neodymium-YAG laser damage thresholds.

Exposures of human volunteers to various lasers are reported. The lasers used were Q-switched neodymium and ruby lasers, a long-pulsed ruby laser, and an argon laser.

A report on the histopathology of retinal injury in rhesus monkeys due to Q-switched neodymium and argon lasers is included.

iii

BLANK PAGE

CONTENTS

ILLUSTRATIONS

The research program whose results are presented in this final report was conducted under contract AF33615-67-C-1752, supported by the USAF School of Aerospace Medicine, Aerospace Medical Division, Brooks Air Force Base, Texas. The project monitor was Lt. Col. J.A. Carpenter.

The research reported covered the period from 15 March 1968 to 15 July 1969. The project leader, Dr. A. Vassiliadis, was responsible for the research activity under SRI Project 7191.

The experiments reported herein were conducted according to the "Principles of Laboratory Animal Care," established by the National Society of Medical Research.

Publication of this report does not constitute Air Force approval of the report's findings or conclusions. It is published only for the exchange and stimulation of ideas.

BLANK PAGE

I INTRODUCTION

The eye is the most vulnerable part of the body to radiation in the visible and near-infrared parts of the spectrum. Specifically, the retina within the eye is particularly vulnerable to intense radiation in this part of the spectrum because of the inherent focusing properties of the ocular system and the transparency of the ocular media. Thus, lasers that emit light in the visible and near-infrared parts of the spectrum are particularly hazardous to the eye, and exposure to their output can cause serious visual loss.

This report identifies thresholds of damage for various lasers. It must be stressed at the outset that these results are based on ophthalmoscopical observations, as are the majority of the threshold measurements that have been reported.[1-6]* Limited studies in the use of histochemical techniques[7,8] have shown that damage can be detected at a somewhat lower level than that required for an ophthalmoscopic observation. Similarly, recent studies in rhesus monkeys[9] have given indications that functional damage occurs at a level only slightly lower than the level obtained by ophthalmoscopically visible reaction.

Thus, it appears that a threshold-of-damage level based on an ophthalmoscopically visible response is not far above the level at which minimal biological response occurs, and that (with appropriate safety factors) safety values can be based realistically on this level.

Because there are considerable differences in the retina and underlying choroid between species, it is necessary to relate the results of animal experiments with human exposures, however limited they may be. Furthermore, even within the same species there are considerable differences in pigmentation. This must be kept in mind, since the human exposures reported herein were made on relatively lightly pigmented Caucasian volunteers.

---

*
References are listed at the end of the report.

This report summarizes the results that have been obtained with various lasers. The majority of the data were obtained in rhesus monkeys, however, some experimental data on human volunteers are included because of the importance of human data in the evaluation of laser damage thresholds in setting safety standards.

The majority of the data were obtained under conditions where small retinal spot sizes were produced. The experimental configuration and procedures have been reported in previous reports.[5,6,8] Rhesus monkey data included for a Q-switched neodymium laser, for a CW argon laser at both the 4880Å and 5145Å lines, and for a CW neodymium-YAG laser. Human exposures are reported for Q-switched neodynium and ruby lasers, for a long-pulsed ruby laser, and for an argon laser.

In addition, the pathology of small laser-induced lesions are discussed. Pathology of retinal lesions, of approximately three times threshold, for both the argon laser and the Q switched Neodyium laser are discussed.

Finally, a brief discussion of laser damage mechanisms is presently based on simple thermal models.

II   RETINAL THRESHOLD DAMAGE FOR PULSED LASERS

A.   General

The experimental methods used in the threshold measurements were based on the simulation of accidental field exposures. Thus, the experimental configuration for retinal damage was designed to provide small retinal spot sizes for lasers in the visible and near-infrared parts of the spectrum.

Retinal laser exposures were made in a special test station[6] constructed around a Zeiss fundus camera. The equipment allows for visual and photographic monitoring before and after each laser exposure and for the measurement of the energy and pulse shape of each laser pulse.

In the laboratory, the laser under experimentation is located between 20 and 25 meters from the test station. Since this distance is optical infinity, the retinal spot size is limited by the eye's optics. At this distance, furthermore, relatively uniform intensity distribution was obtained over the pupil of the eye. In addition, because of the distance to the laser, and the small size of the laser aperture, the beam used in the experiments was sufficiently well collimated that the eye's optics were the limiting factor on the size of the retinal image.

The retinal spot size obtained in each eye was estimated by the use of a CW He-Ne laser beam of cross section equal to that used for the pulsed laser; the size of the retinal spot was estimated by taking photographs of the retinal image; from these were obtained microdensitometer traces of the images.

The refractive error for each eye of the experimental animals was determined with a retinoscope and neutralized by mounting the appropriate corrective lens in front of the eye. Thus, each eye was exposed to the laser in such a way as to minimize the retinal spot size in the visible part of the spectrum. However, for the neodymium laser, at 1.06μ ($10600\text{\AA}$), there is a refractive error due to changes in the refractive

index of the ocular media. Thus, for the neodymium laser, data were obtained for two cases: In the first, the correction for the visible spectrum was used, and in the second, additional correction was added for better focus of the neodymium wavelength.

Most of the data obtained in the rhesus monkeys are for the para-macular areas, i.e., the area around the macula. A small amount of data were obtained in the macular area. This is important for two reasons: First, the macular area is more pigmented than the rest of the fundus and therefore more vulnerable to light damage, and, second, the macula is the site of acute, central vision.

The experimental configuration in the human experiments was identical to that used in the rhesus monkey experiments. The seven human volunteers were carefully refracted, and the appropriate prescribed lens was used in front of the experimental eye. The left eye of each volunteer was used, and a few exposures were made on the nasal side of the optic nerve. Thus, all the exposures were made well away from the macula in an area about 25° from the optic axis.

In all the experiments, damage to the retina was based on the criterion of a visible change as seen with the ophthalmoscope at the site of a laser impact within one hour of the exposure.

B.   Q-Switched Neodymium Laser Experiments in Rhesus Monkeys

In this program, extensive data were obtained on the Q-switched neodymium laser. The laser used had a pulse of approximately 30 ns and was located sufficiently far away from the experimental test station that the retinal spot size was predominantly determined by the eye optics of the experimental animal.

The experimental animal eyes were refracted to the nearest 0.25 diopter prior to each experiment. The corrective refractive lens was then placed in front of the eye and eight exposures were made above the macula and four exposures were made in the macula. The retinal spot size was not minimal for the neodymium wavelength, for these exposures, since the animal was refracted by retinoscope in the visible part of the

spectrum. An additional 1/2 to 3/4 diopter was added to the refractive lens, depending on the judgment of the nearest 0.25 diopter that was made on the refraction. Eight laser exposures were then made in the paramacular area below the macula. In this way three sets of data were obtained in each eye used in the experiments.

The data for the paramacula area without the additional correction are summarized in Figure 1. The individual exposures are classified according to whether or not a lesion was observed, and are plotted as a function of total energy into the eye. The energy scale is then divided into equal logarithmic intervals, and a probability for damage for each interval is calculated, i.e., the number of exposures that caused observable response divided by the total number of exposures within the interval. The histogram is then obtained and a smooth curve is drawn through the histogram, indicating the probability curve that might be obtained for a sufficiently large sample. The spread in the data is attributed to variations in pigmentation within the same retina and between different animals, and by the fact that the spot size is different in each eye. The spot sizes in the Q-Switched neodymium experiments were calculated based on microdensitomer traces of HeNe laser photographs and on extrapolation to the 10600Å wavelength. The average spot size calculated for the rhesus monkeys for these experiments was 90μ. The 50 percent probability for damage is found to be approximately $290\mu J$.

The data in the macular area were taken without the additional correction so that the average retinal spot size is also approximately 90μ. The data for the macular area are summarized in Figure 2. The 50-percent probability for damage for the macular area is found to be about $150\mu J$. Thus, there is apparently a factor of two more sensitivity in the macular area compared with the paramacular area.

The data for the case where the neodymium laser was more accurately focused on the retina, by adding an additional corrective lens, are summarized in Figure 3. The estimate average spot size for these exposures is 60μ. The 50-percent probability for damage for this case is seen to be approximately $220\mu J$, which represents a surprisingly small

5
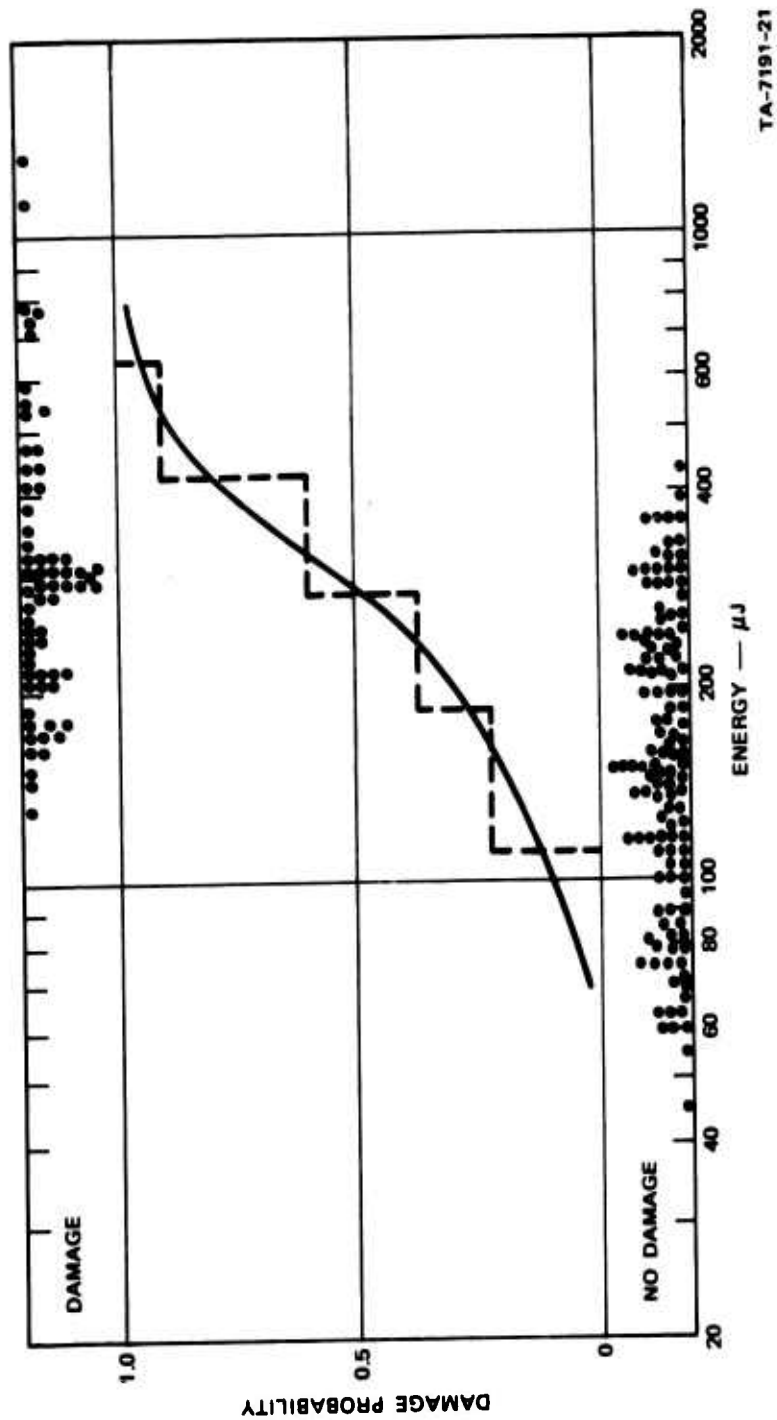
FIGURE 1   RETINAL DAMAGE IN RHESUS MONKEY PARAMACULAR AREA FOR Q-SWITCHED NEODYMIUM LASER

6
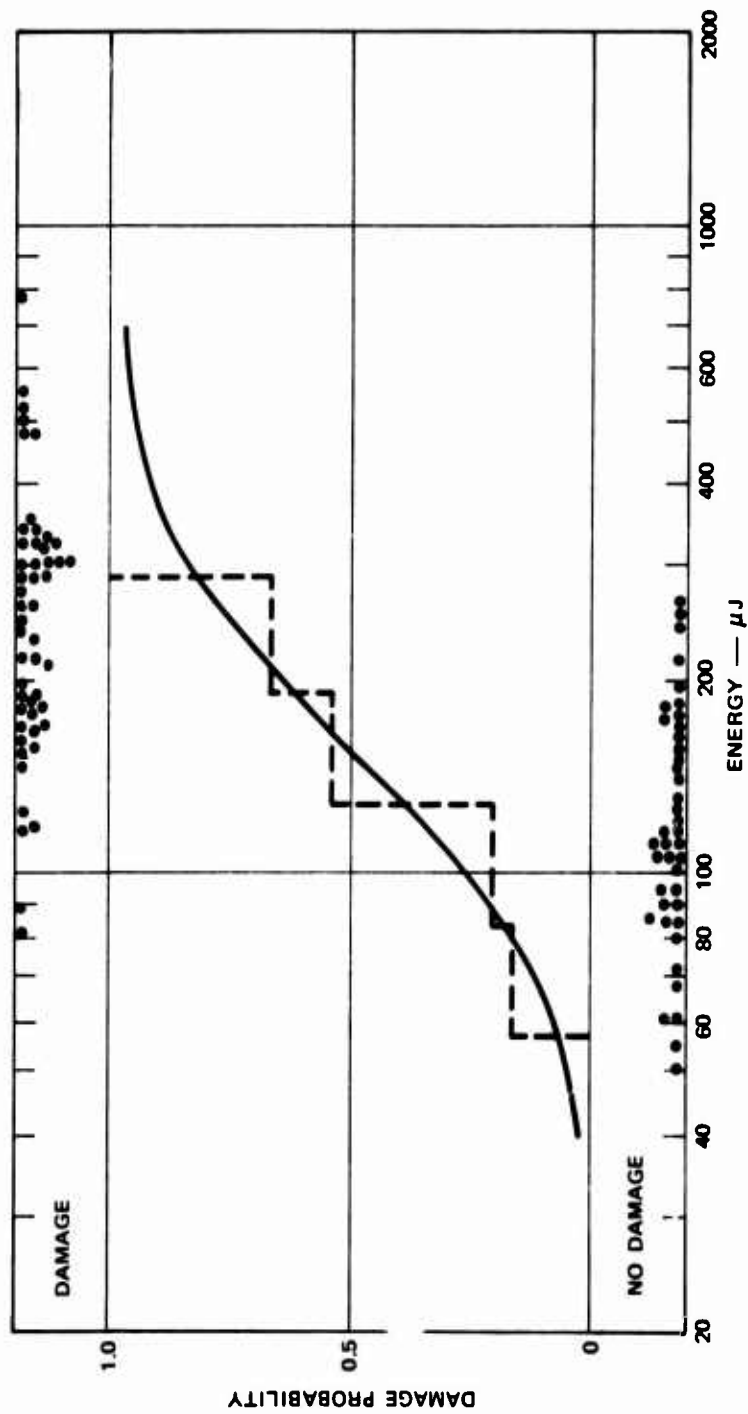
FIGURE 2   RETINAL DAMAGE IN RHESUS MONKEY MACULAR AREA
FOR Q-SWITCHED NEODYMIUM LASER

TA-7191-22

7
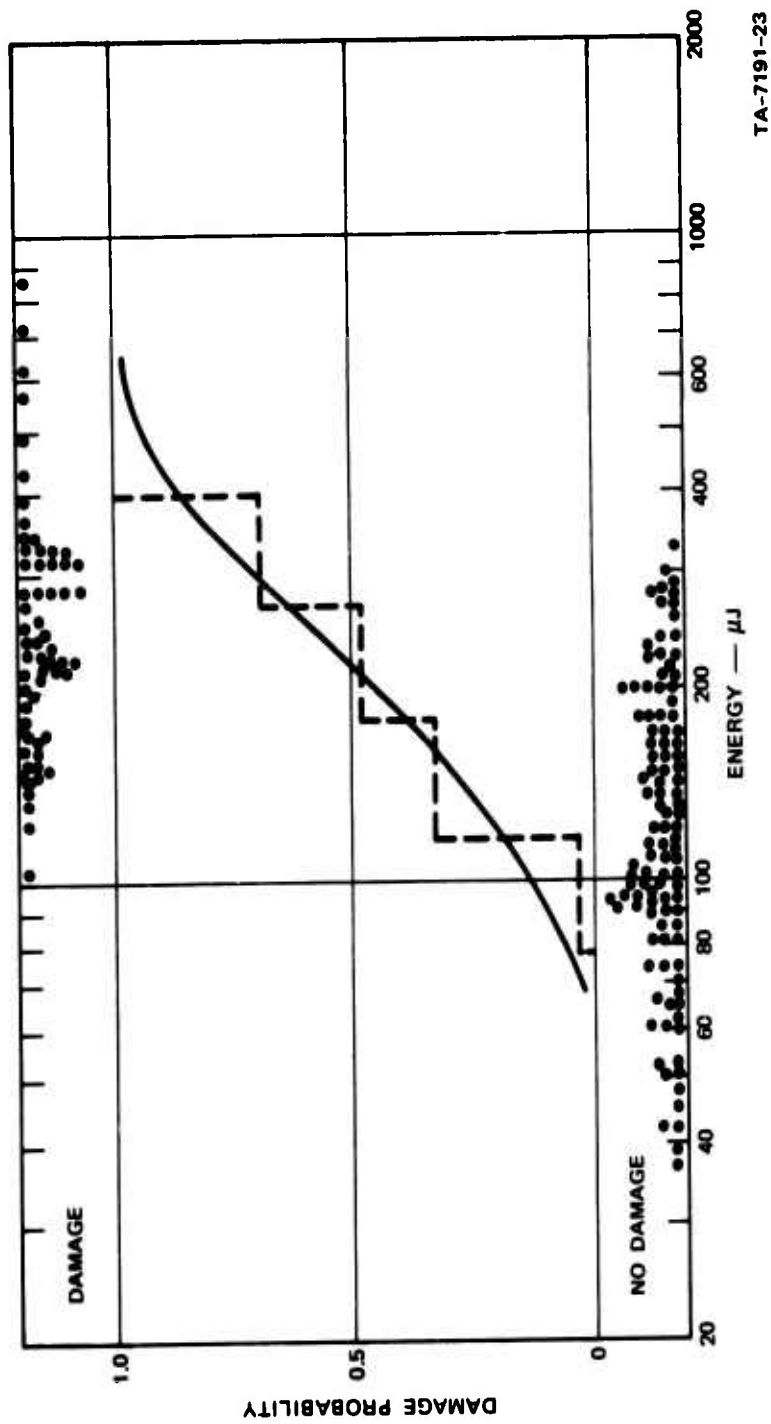
FIGURE 3   RETINAL DAMAGE IN RHESUS MONKEY PARAMACULAR AREA
FOR Q-SWITCHED NEODYMIUM LASER WITH ADDITIONAL ≈ 5/8
DIOPTER CORRECTION

TA-7191-23

8

reduction from the 290µ J obtained for the case where no correction was made for the neodymium wavelength.

This small change in total threshold energy for an appreciable change in retinal spot size is difficult to explain in view of the fact that, for Q-switched exposures, negligible thermal relaxation of the exposed site can take place and thus the threshold energy density should be independent of spot size. Similar effects have been reported previously by other investigators.[4,10] In a later section, a similar anomaly is shown to exist in the argon laser data taken as a function of spot size. On the other hand, an in vitro study[10] has shown no such anomaly for Q-switched laser damage to pigment cells. Thus, the effect must be due to a pecularity of the ocular media or to the method of observation or detection of the threshold lesions.

One argument that has been proposed[11] to explain this effect regards the visibility of lesions as a function of image size and argues that a small lesion must be more severe than a large one in order to be detected by the observer. However, since this model predicts negligible effects for lesions above 50µ, it is difficult to see how this explanation can provide a sufficiently strong argument, particularly in view of the fact that the variations that are observed in the literature begin at spot sizes of about 500µ.

One possible explanation for this phenomenon is that it is caused by the scattering of the refracting surfaces and media of the ocular system. The scatter would be expected to be primarily in the forward direction so that the effect would be more pronounced for the small spot sizes and negligible for the large spot sizes. Thus the peak energy density for small spot sizes at the retina would be appreciably less than that calculated based on transmission measurements of the ocula media.

The data for the Q-switched Neodymium laser damage in rhesus monkeys is summarized in Table I, where an "effective" retinal energy density is also shown.

Table I

Q-SWITCHED NEODYMIUM LASER DAMAGE THRESHOLDS IN RHESUS MONKEYS

Condition	Retinal Area	No. of Eyes	50 Percent Probability For Damage	
			Total Energy	Effective Retinal Energy Density
Uncorrected for 1.06 μ	Paramacular	24	290μ J	4.6 J/cm^2
Uncorrected for 1.06μ	Macular	24	150μ J	2.4 J/cm^2
Corrected for 1.06μ	Paramacular	24	220μ J	7.6 J/cm^2

Effective retinal energy density is calculated by taking the total energy entering the eye at the cornea and dividing it by the estimated retinal spot size area. Thus, this is not the true retinal energy density, since the losses due to the intervening ocular media are not taken into account.

C. Pulsed Laser Experiments in Human Volunteers

1. General Remarks

This section contains a summary of data obtained on seven human volunteers with heathly eyes and a comparison with data previously obtained in rhesus monkeys. It must be emphasized--and the data bring this out--that the variations in pigmentation of the fundus will cause variations in the threshold for damage. The human data that are reported were obtained in relatively lightly pigmented Causasian eyes.

The exposures were made on the nasal side of the disc, a factor that must be kept in mind when comparison is made with the rhesus monkey data, since the rhesus data were gathered in paramacular areas on the temporal side of the disc. This might be important if the pigmentation in the fundus has a different character at this location as compared to the macula. The lesions were placed in the area of about 25° from the optic axis.

10

The experimental configuration used in the human experiments was identical to that used in rhesus monkey experiments. In all cases the pulsed laser was kept at as large a distance from the experimental station as possible consistent with the required levels for exposure. In all but the highest two exposures of the neodymium Q-switched laser, this distance was sufficient to make the eye optics the limiting factor in spot size determination. In the highest two neodymium laser exposures, the distance of the laser was only about 6 meters. However, since the eye was not focused for the neodymium wavelength, the retinal spot size is estimated to be of the order of 90μ.

2. Q-Switched Neodymium Laser Exposures

The first series of experiments on healthy human subjects were undertaken using a Q-switched neodymium laser with a 30-ns pulse length. In these experiments, the human volunteers were carefully refracted, and the appropriate prescribed lens was used in front of the experimental eye. This means that at the neodymium wavelength, the retinal image is not minimum but is of the order of 90μ.

The left eye of each volunteer was used, and several exposures were made on the nasal side of the optic nerve. Thus, all the exposures were well away from the macular area.

The data for the human retinal exposures are shown in Figure 4. Here it is seen that large number of exposures were made around the value of 45μJ, since this is the USAF-recommended safe level. It is surprising that no damage was observed until a level of about 4mJ total energy was reached. At this level, the minimum lesion observed took 25 minutes to develop, while at 7mJ an immediate small lesion was seen. These lesions are the only ones that were seen, even under careful slit-lamp examination of all exposure sites. Both these lesions had completely disappeared when examined six days later, and could not be seen under slit-lamp examination. Figure 5 shows the area of the retina before exposure, Figure 6 shows the two small lesions observed, and Figure 7 shows the area six days after exposure.

FIGURE 4   HUMAN RETINAL EXPOSURES WITH Q-SWITCHED NEODYMIUM LASER—PULSE LENGTH 30 ns

TA-7191-17

12
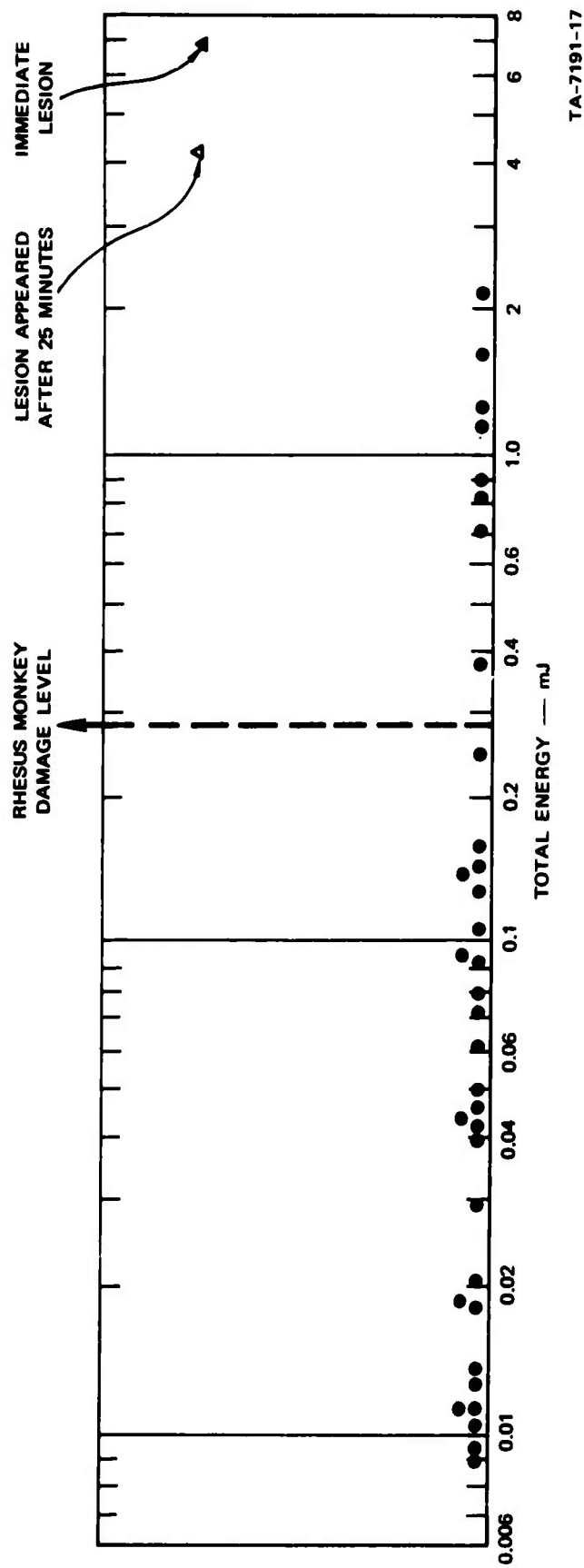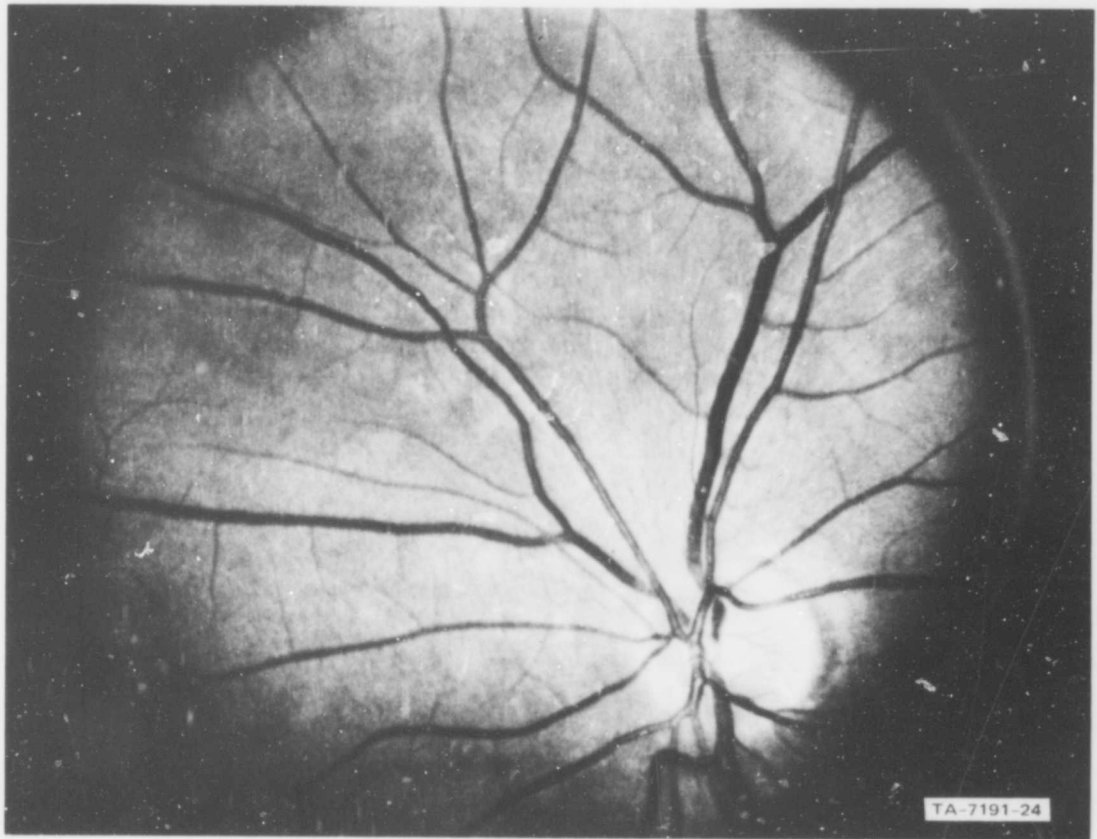
FIGURE 5   HUMAN FUNDUS PRIOR TO EXPOSURE WITH Q-SWITCHED NEODYMIUM LASER

The spot size in the eye that received the highest exposure was measured at the He-Ne wavelength. The procedure has been described previously and makes use of photography of the retinal image and the use of microdensitometer to measure the images. Thus, at the He-Ne wavelength, the spot size on the retinal was calculated to be 30μ. However, since the neodymium wavelength is not completely focused when the eye is properly refracted for the visible region, the spot size for 1.06μ was estimated to be approximately 90μ.

A comparison of the human data and the rhesus monkey data is made in Table II,

13
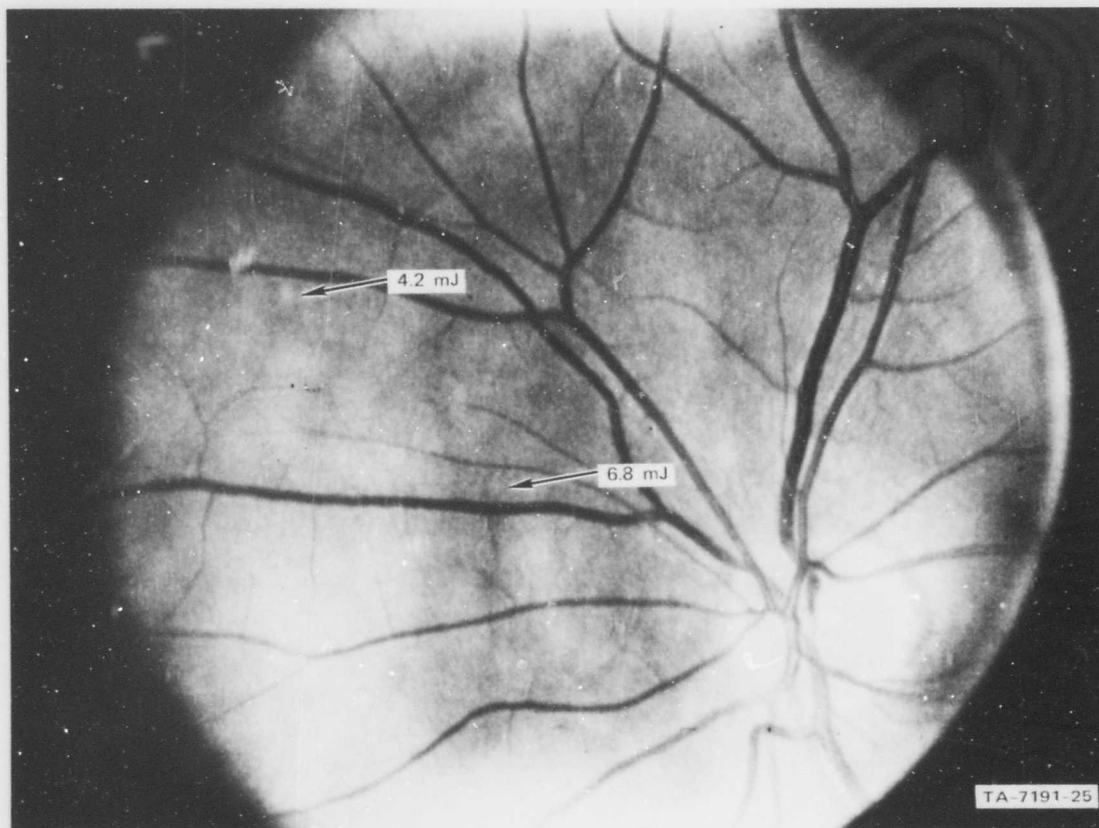
FIGURE 6   HUMAN FUNDUS SHOWING LESIONS 30 MINUTES AFTER EXPOSURE
TO Q-SWITCHED NEODYMIUM LASER

Table II

Q-SWITCHED NEODYMIUM LASER DATA

Species	No. of Eyes	Pulse Length	No. of Data Points	Lowest Energy for Observed Damage	Energy for 50% Probability for Damage
Rhesus	24	30 ns	194	140μ J	290μ J
Man	5	30 ns	37	4.2mJ	insufficient data

where it is seen that the level where damage was first observed in the
human eye was appreciable higher than the lowest observed in the rhesus
monkey.

14
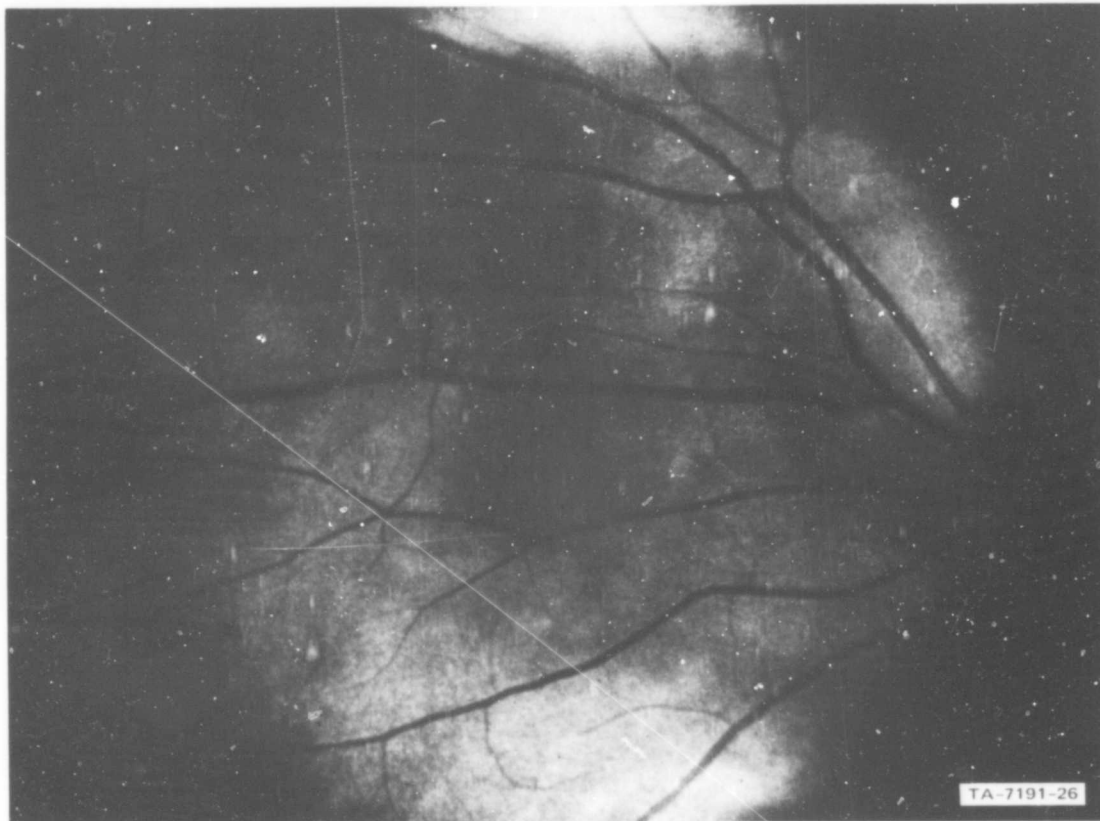
FIGURE 7   HUMAN FUNDUS SIX DAYS AFTER EXPOSURE TO Q-SWITCHED NEODYMIUM LASER

3.   Q-Switched Ruby Laser Exposures

In experiments similar to those of the Q-switched neodymium laser, a Q-switched ruby with a 20-ns pulse length was used to obtain some data on two human subjects.

The data are summarized in Figure 8 where it is seen that a number of lesions were obtained. These exposures were made in two volunteer eyes. Again these lesions had completely disappeared when examined in a few days and could not be found under slit-lamp examination. An
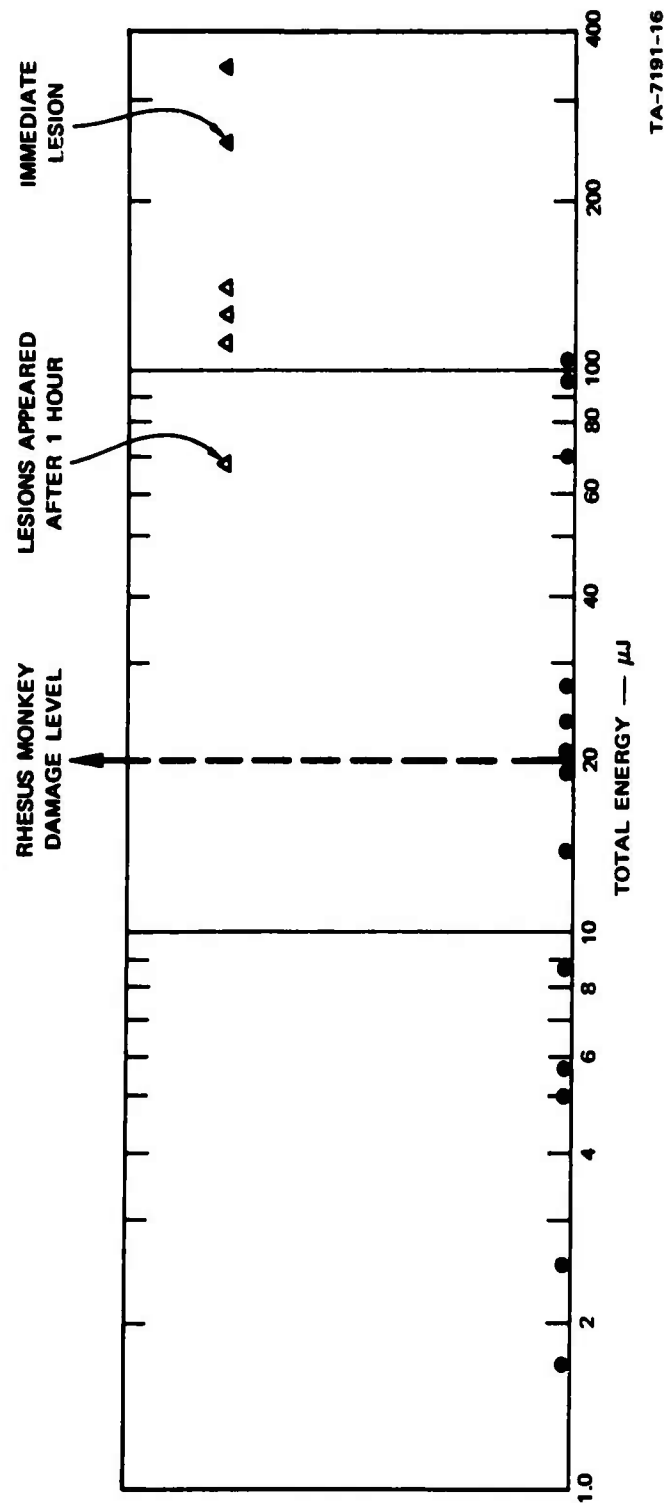
FIGURE 8   HUMAN RETINAL EXPOSURES WITH Q-SWITCHED RUBY LASER—PULSE LENGTH 20 ns

16

example showing three lesions is shown in Figure 9. The spot size measured with the He-Ne laser was found to be 25μ in this eye.

A comparison of the data with rhesus monkey data[8] obtained with another laser is made in Table III. The spot sizes achieved in the rhesus monkeys ranged from 25μ to 75μ with a mean of approximately 50μ. The data was taken with pulses of different length; however, since both pulses are considerably shorter than any thermal relaxation processes in the fundus, the differences observed may be attributed solely to species differences. Again, the human data are seen to be higher than the rhesus monkey data.
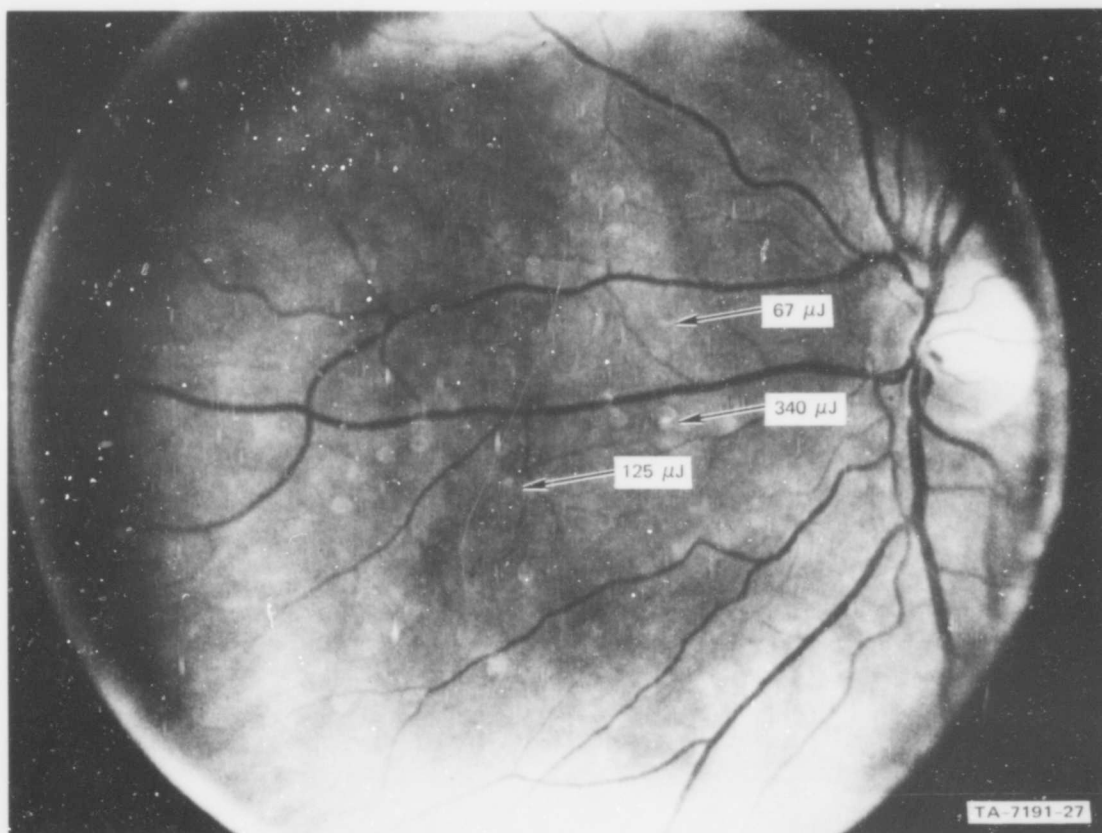
FIGURE 9   HUMAN FUNDUS SHOWING LESIONS ONE HOUR AFTER EXPOSURE
TO Q-SWITCHED RUBY LASER

17

Table III

SUMMARY OF Q-SWITCHED RUBY LASER (6943Å) DATA

Species	No. of Eyes	Pulse Length	No. of Data Points	Lowest Energy for Observed Damage	Energy for 50% Probability for Damage
Rhesus	10	10 ns	72	$8.6\mu J$	$22\mu J$
Man	2	20 ns	19	$68\mu J$	Insufficient Data

4. <u>Long-Pulse Ruby Laser Exposures</u>

In a brief experiment involving a single human volunteer, a number of exposures were made using a long-pulse ruby laser with a pulse duration of 200µs.

The data obtained in the one human volunteer are presented in Figure 10; only the two lesions were seen. A photograph of the lesions is shown in Figure 11. Again these lesions had disappeared when the retina was re-examined after a week.

A comparison with some threshold data that were recently taken in rhesus monkeys on another project is made in Table IV. Here again, an appreciable difference may be noted between the two species.

Table IV

SUMMARY OF LONG-PULSE RUBY LASER 6943Å DATA

Species	No. of Eyes	Pulse Length	No. of Data Points	Lowest Energy for Observed Damage	Energy for 50% Probability for Damage
Rhesus	8	$200 \mu s$	135	0.048mJ	0.08mJ
Man	1	$200 \mu s$	9	0.95mJ	Insufficient Data

18
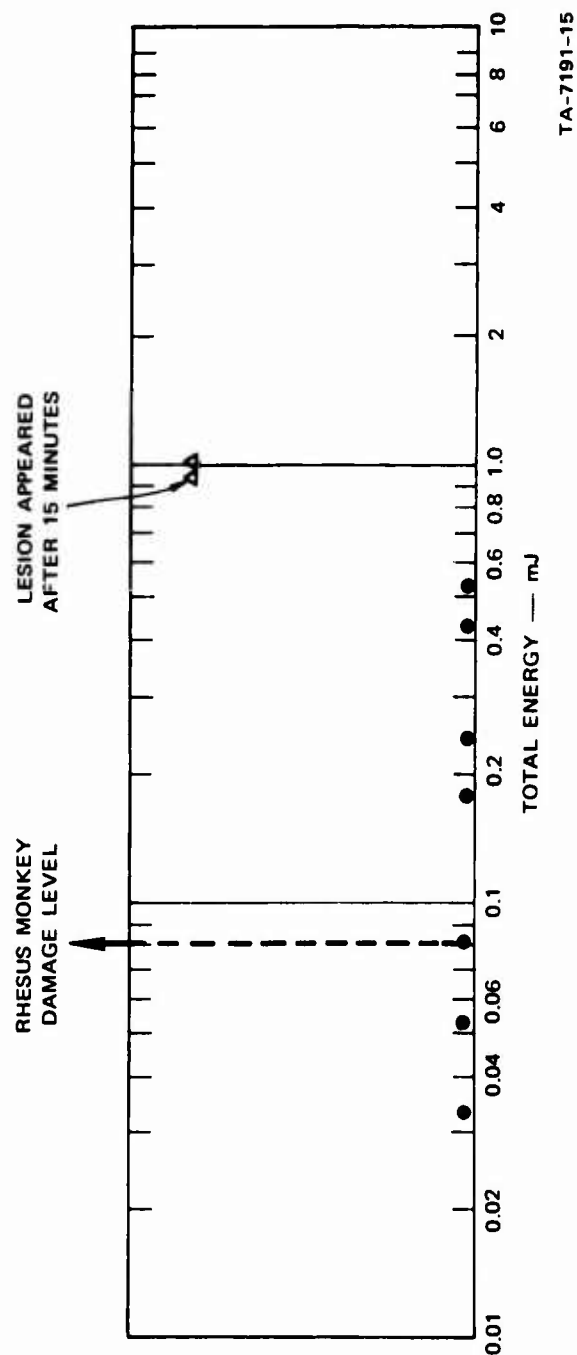
FIGURE 10   HUMAN RETINAL EXPOSURES WITH LONG-PULSED RUBY LASER—PULSE LENGTH 200 μs

19
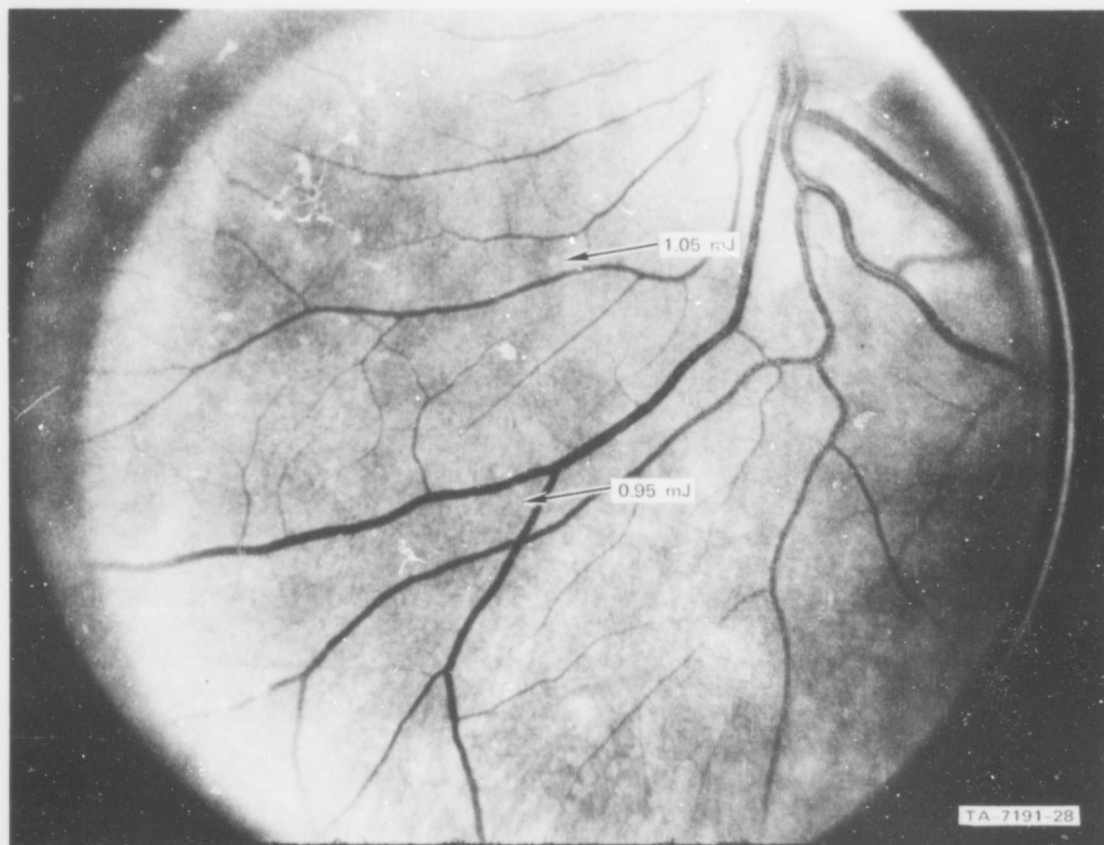
FIGURE 11   HUMAN FUNDUS SHOWING LESIONS ONE HOUR AFTER EXPOSURE
TO LONG-PULSED RUBY LASER

20

III RETINAL DAMAGE FROM CW LASERS

A. Genera1

The experimental configuration for the CW laser exposures was such
that the retinal spot size could be minimized. Data were taken for
three CW lasers: the argon laser, He-Ne laser, and the neodymium-YAG
laser. The large majority of the data were taken at small retinal spot
sizes; however, some data for the argon laser were taken at larger spot
sizes. The data reported in this section were taken in the paramacular
area.

The beam of the CW lasers was expanded sufficiently so that the
intensity variation across the entrance iris of the experimental con-
figuration was no more than 20 percent across the beam. Two argon
lasers were used in the experiments--a Spectra Physics Model 140 and a
Coherent Radiation Labs Model 52. The He-Ne laser was a Spectra-Physics
Model 125, kindly loaned to SRI by Spectra-Physics for this brief experi-
ment. The neodymium-YAG laser was a Korad Model KY-1.

The experiments were carried out in the terminal test station,
built around a Zeiss fundus camera, described in previous reports.[6]

The experiments for retinal damage were made using a 4-mm aperture
to limit the size of the beam entering the eye. The shutter on the test
station was used to obtain various exposure times. The shutter was
calibrated by actuating it a number of times and measuring the signal
detected at the monitor. The exposure times were taken as the average
of ten observations. The variations in time from one exposure to
another were within 5 percent.

The experimental animals were given 1 percent atropine for five
days prior to the day of exposure. This was done to minimize the vari-
ations of retinal spot size due to slight changes in accommodations.
The eyes were refracted with a retinoscope prior to experimentation, and
the appropriate lens was placed in front of the eye during the exposures
to the laser beam.

21

Because the refraction is made in white light, the correction required for the argon laser and for the He-Ne lasers will be somewhat off from the measured correction. Since the refraction cannot easily be made to an accuracy of less than ±0.25 diopter, it was decided to use simply the measured refractive error.

The retinal spot size for the lasers was estimated by photographing the retinal image through the Zeiss fundus camera. Microdensitometer traces were then obtained and the retinal spot size estimated by assuming a focal length for the eye.

B.   Argon Laser Experiments

1.   Rhesus Monkey Exposures

As outlined in the previous section, the majority of the data were obtained under the conditions in which the retinal spot size was minimized. The animal's eye was refracted with a retinoscope and the proper lens was placed in front of the eye. For some animals, however, larger reti al spots were made by diverging the laser beam.

Data at minimum spot sizes were obtained for exposure times of 1.5, 4.4, 13.5, 80, .250, and 960 ms. The average spot size for these exposures was approximately 30μ. Limited data were obtained for a 200μ retinal spot size for exposure times of 13.5, 80, 400, and 1600 r⁻ ᵗ.   ᵤre obtained for a 100μ retinal spot size for a 80ms exposure t. .

The data for the small retinal spot sizes are summarized in Table V and plotted in Figures 12 to 20. Here it is observed that one point (the 13.5 ms) of the 5145Å data appears to be too high. Examination of the actual data plot shown in Figure 19 shows that data were not taken at sufficiently low levels. Thus, because of insufficient low data points with no damage, the 50 percent point was not accurately determined.
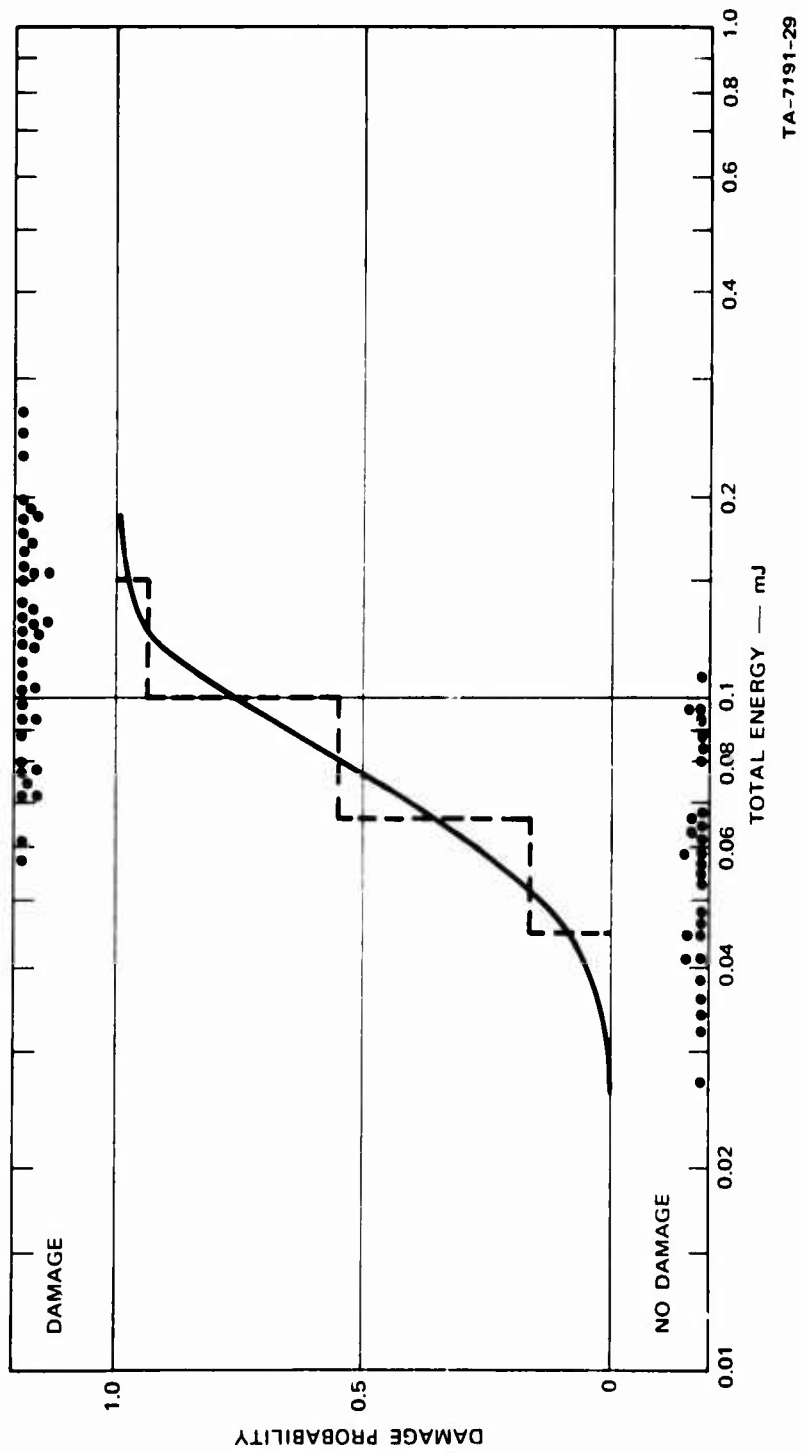
FIGURE 12   DAMAGE TO RHESUS MONKEY RETINA WITH ARGON LASER—1.5 ms, 4880 Å

23
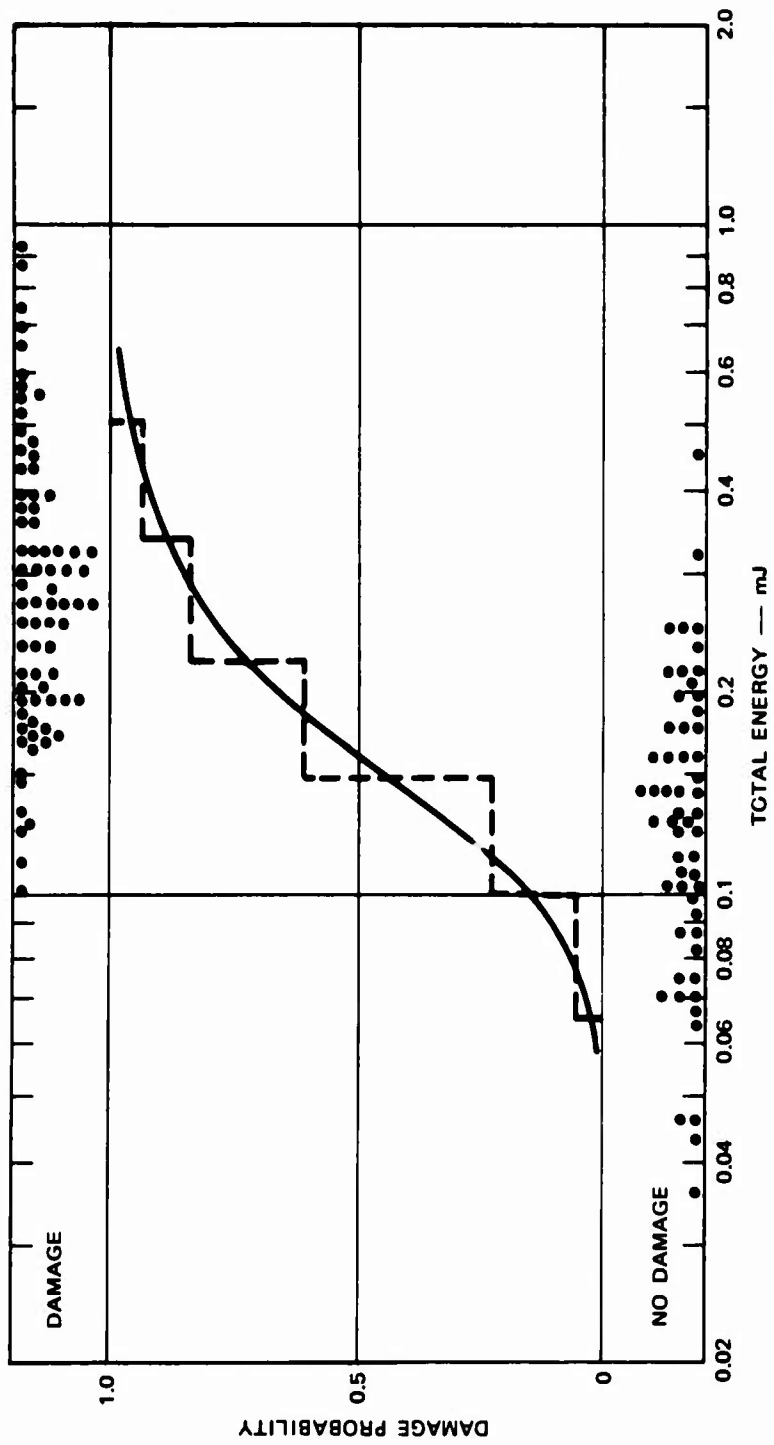
FIGURE 13   DAMAGE TO RHESUS MONKEY RETINA WITH ARGON LASER—4.4 ms, 4880 Å

24
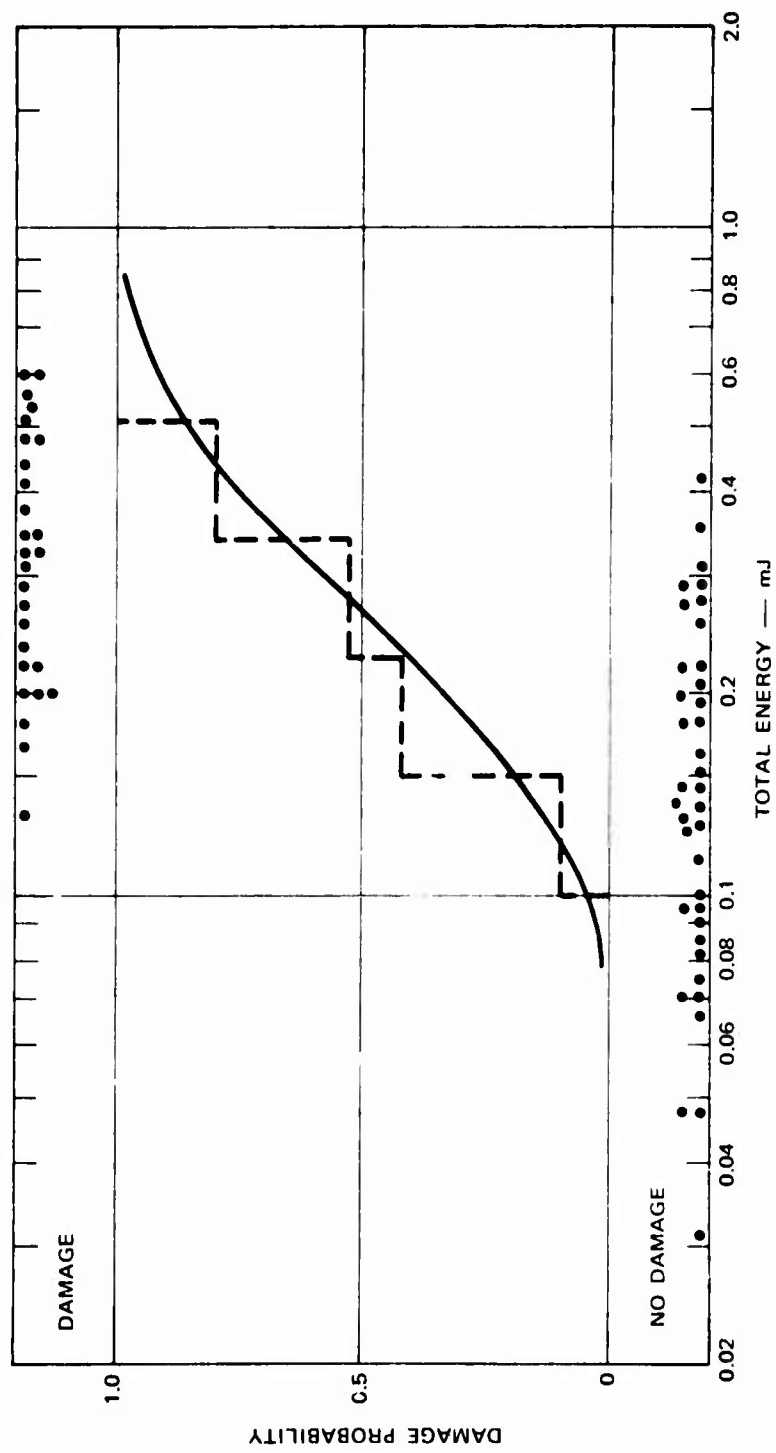
FIGURE 14   DAMAGE TO RHESUS MONKEY RETINA WITH ARGON LASER—13.5 ms, 4880 Å

25
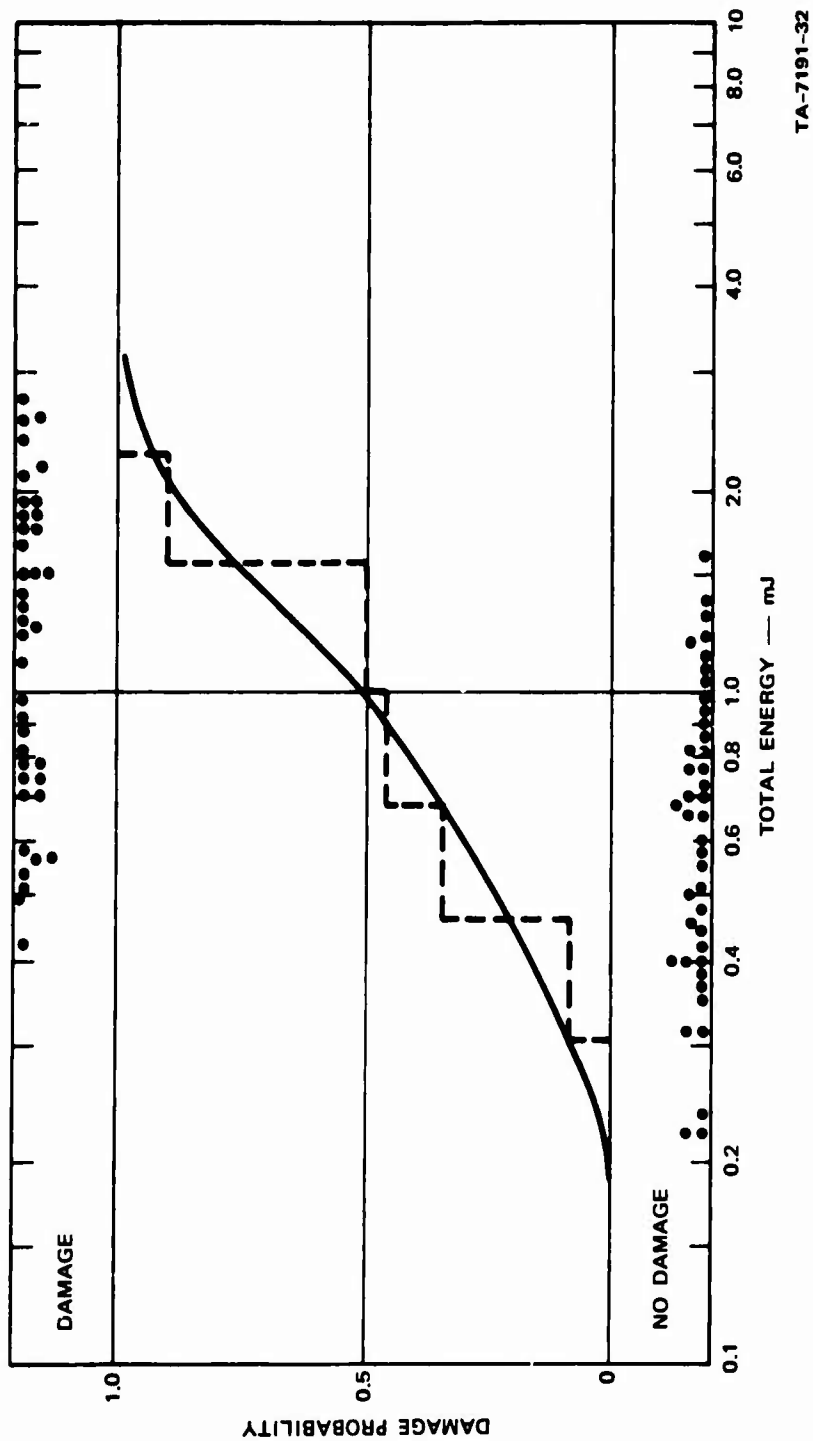
FIGURE 15   DAMAGE TO RHESUS MONKEY RETINA WITH ARGON LASER—80 ms, 4880 Å

TA-7191-32

26
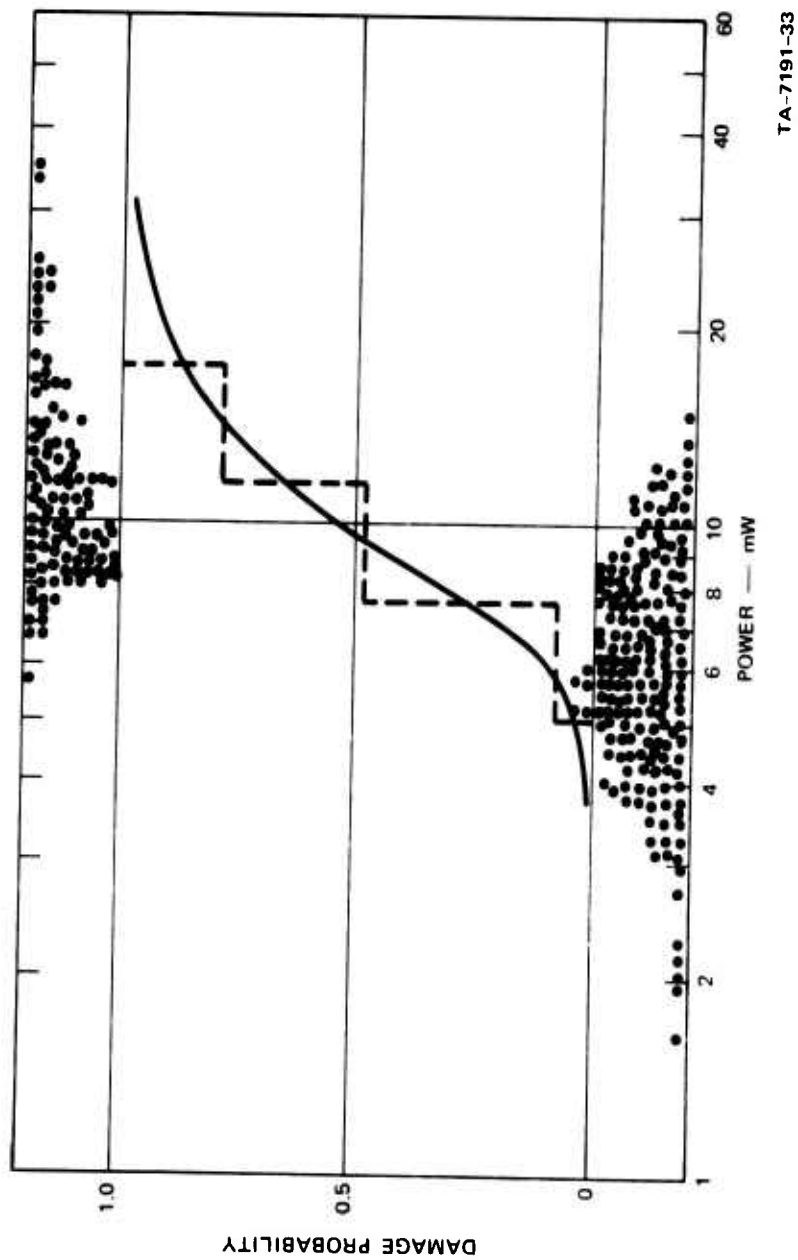
FIGURE 16   DAMAGE TO RHESUS MONKEY RETINA WITH ARGON LASER—250 ms, 4880 Å
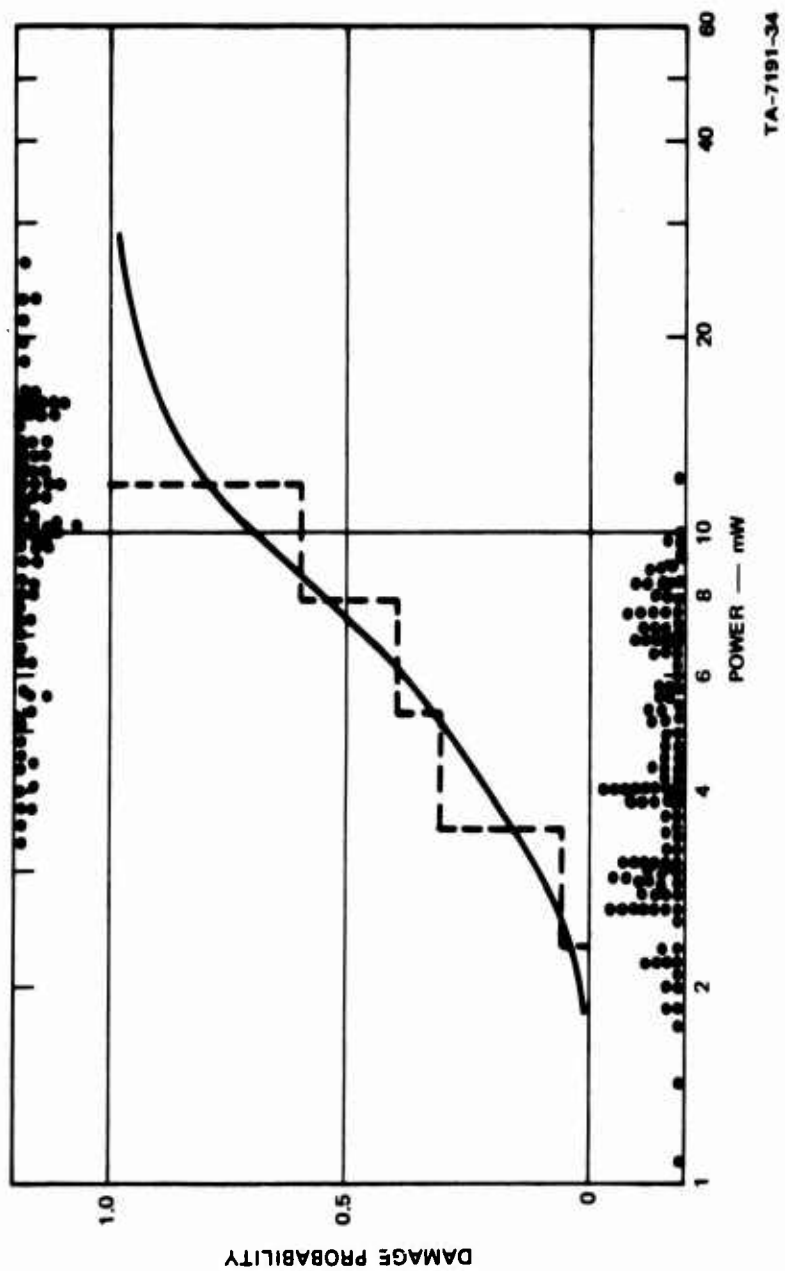
TA-7191-33

FIGURE 17   DAMAGE TO RHESUS MONKEY RETINA WITH ARGON LASER—960 ms, 4880 Å

28
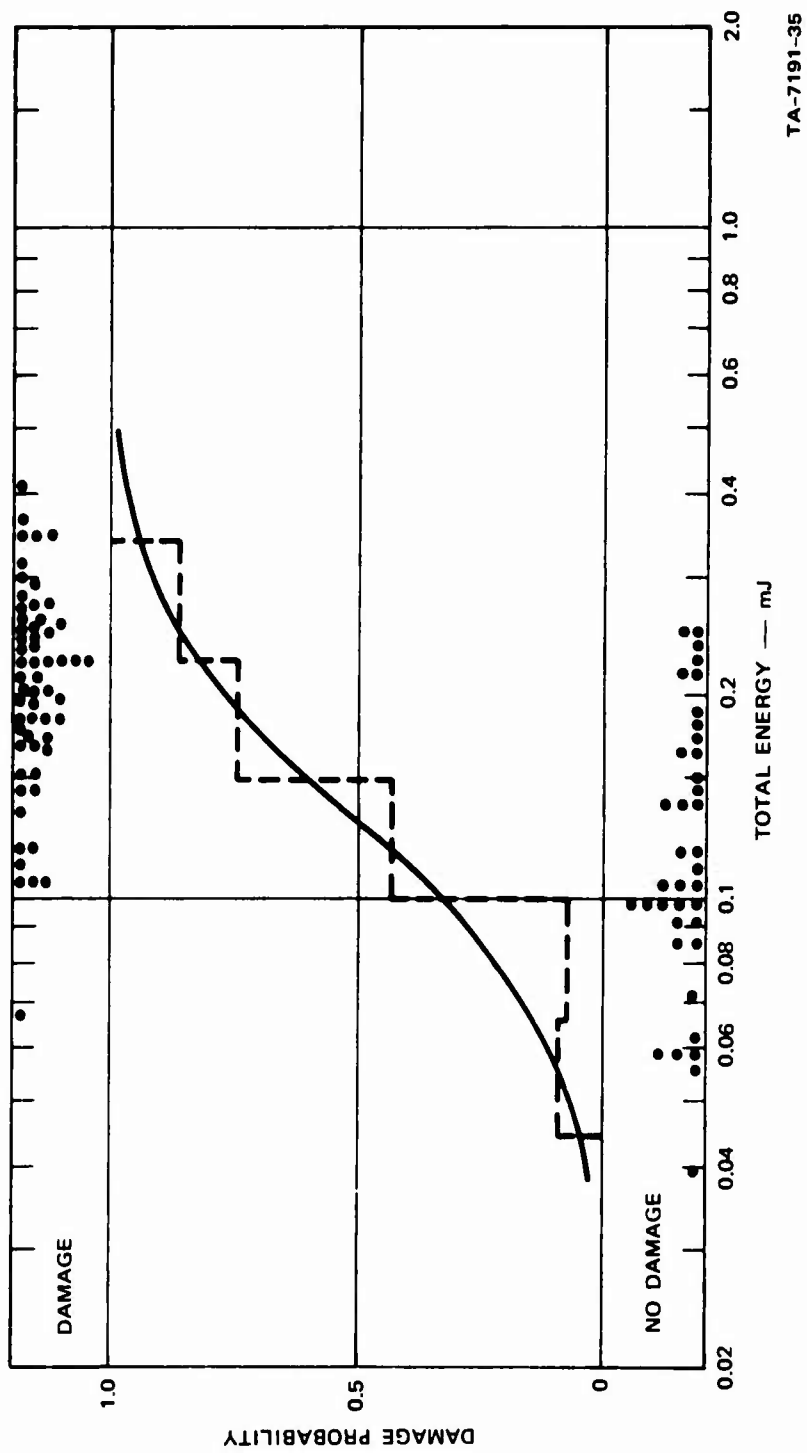
FIGURE 18 DAMAGE TO RHESUS MONKEY RETINA WITH ARGON LASER—4.4 ms, 5145 Å

29
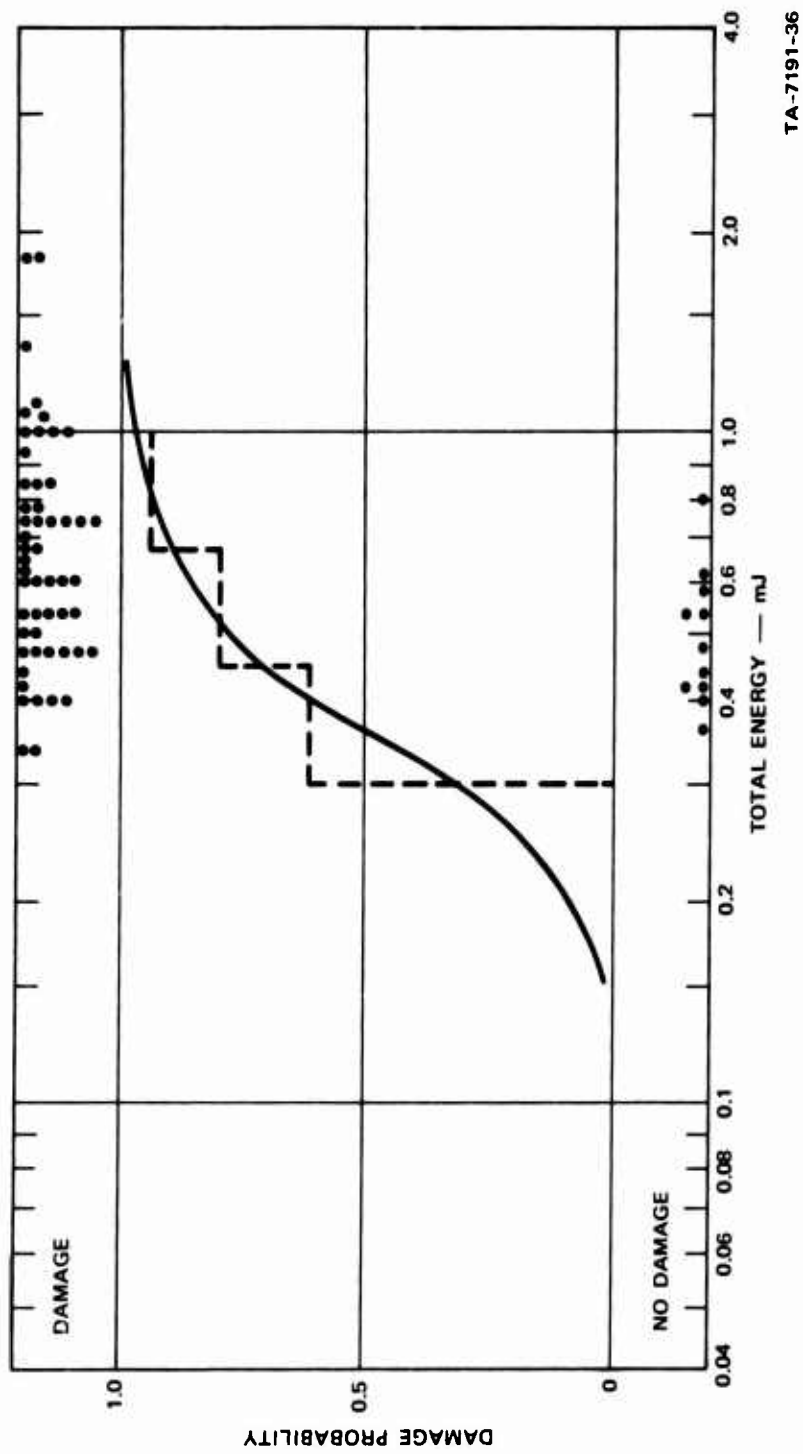
FIGURE 19   DAMAGE TO RHESUS MONKEY RETINA WITH ARGON LASER—13.5 ms, 5145 Å

TA-7191-36

30
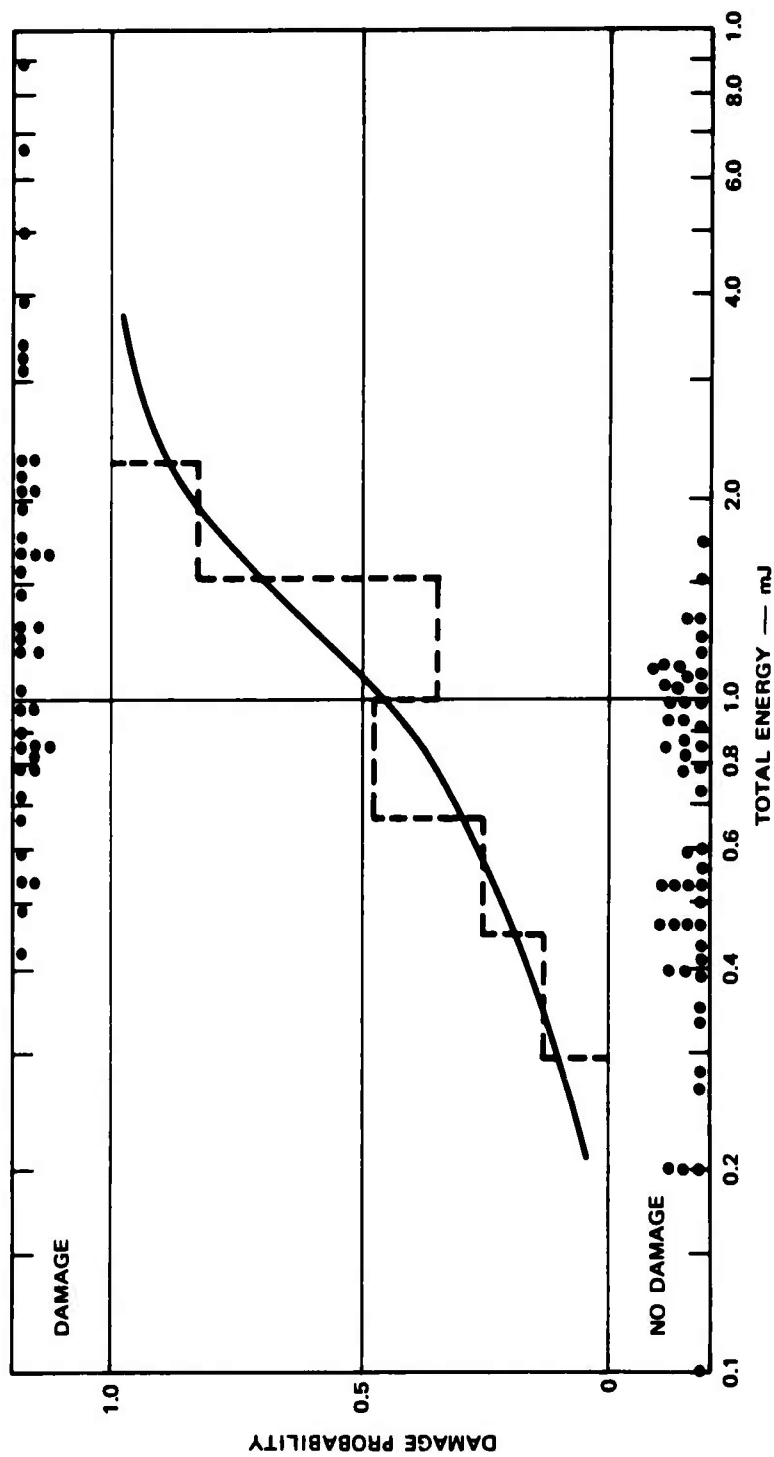
FIGURE 20   DAMAGE TO RHESUS MONKEY RETINA WITH ARGON LASER—80 ms, 5145 Å

31

Table V

SUMMARY OF ARGON LASER EXPOSURE WITH

SMALL SPOT SIZES IN RHESUS MONKEYS

Wavelength (Å)	Time (ms)	No. of Eyes	Lowest Power for Observed Damage (mw)	Power for 50% Damage Probability (mw)
4880	1.5	4	39	51
	4.4	8	23	36
	13.5	4	10	20
	80	6	4.7	13
	250	24	5.7	9.5
	960	12	3.4	7.4
5145	4.4	6	15	30
	13.5	4	2.4	27
	80	6	5.4	14

The 200μ and 100μ retinal spot size data, are summarized in Table VI and shown in Figures 21, 22 and 23. It is apparent that the

Table VI

SUMMARY OF ARGON LASER EXPOSURES AT 200μ AND

100μ SPOT SIZES IN RHESUS MONKEYS (4880Å)

Spot Size (μ)	Time (ms)	No. of Eyes	Power for 50% Probability for Damage (mw)
200	13.5	2	48
	80	4	34
	400	4	24
	1600	4	19
100	80	4	22

data for the larger spots give much sharper transitions from damage to no damage. This is due primarily to the fact that the spot size is more consistent from one eye to another.

32
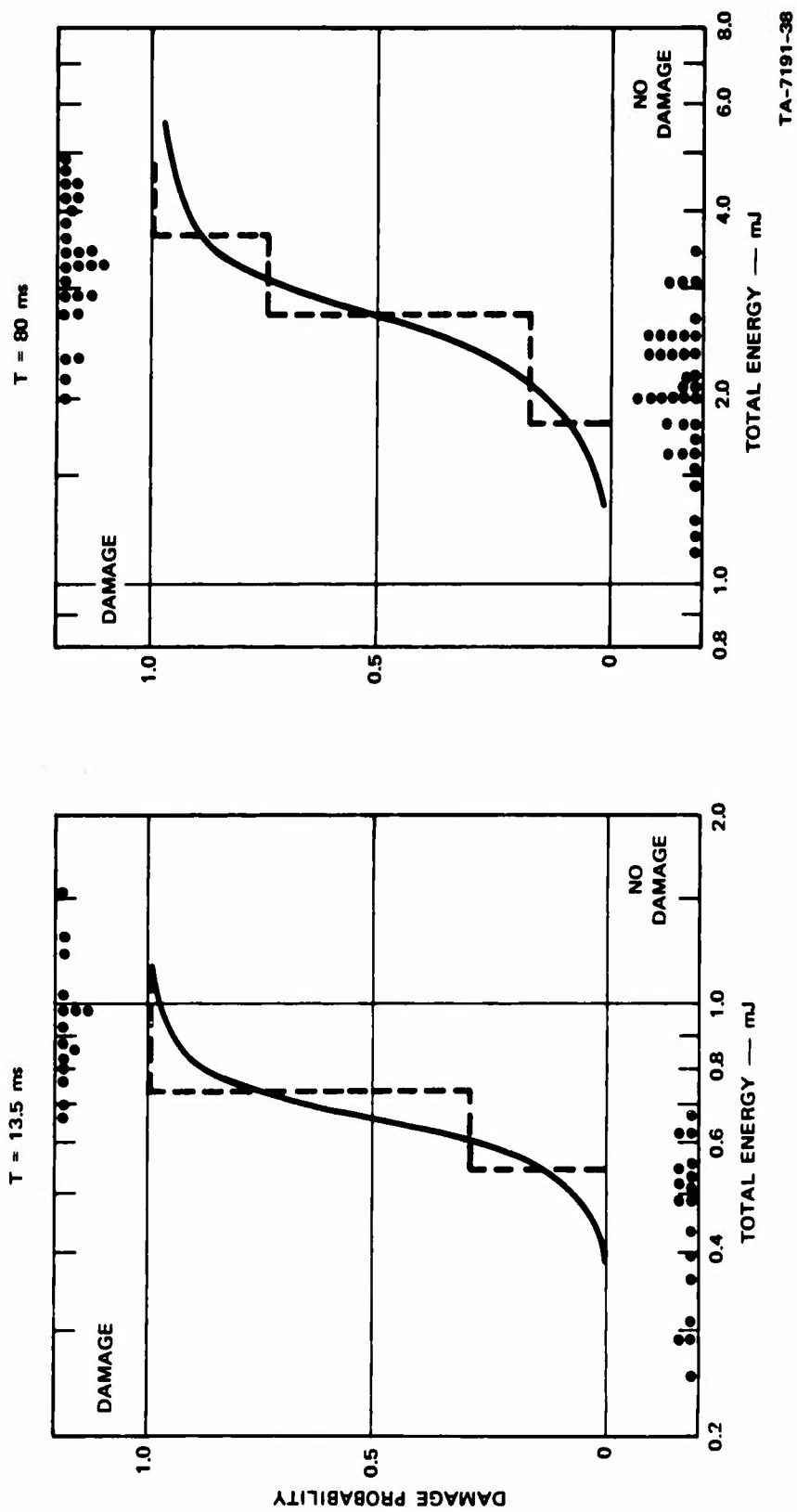
FIGURE 21 DAMAGE TO RHESUS MONKEY RETINA WITH ARGON LASER—13.5 AND 80 ms,
4880 Å, 200-μ RETINAL SPOT

33
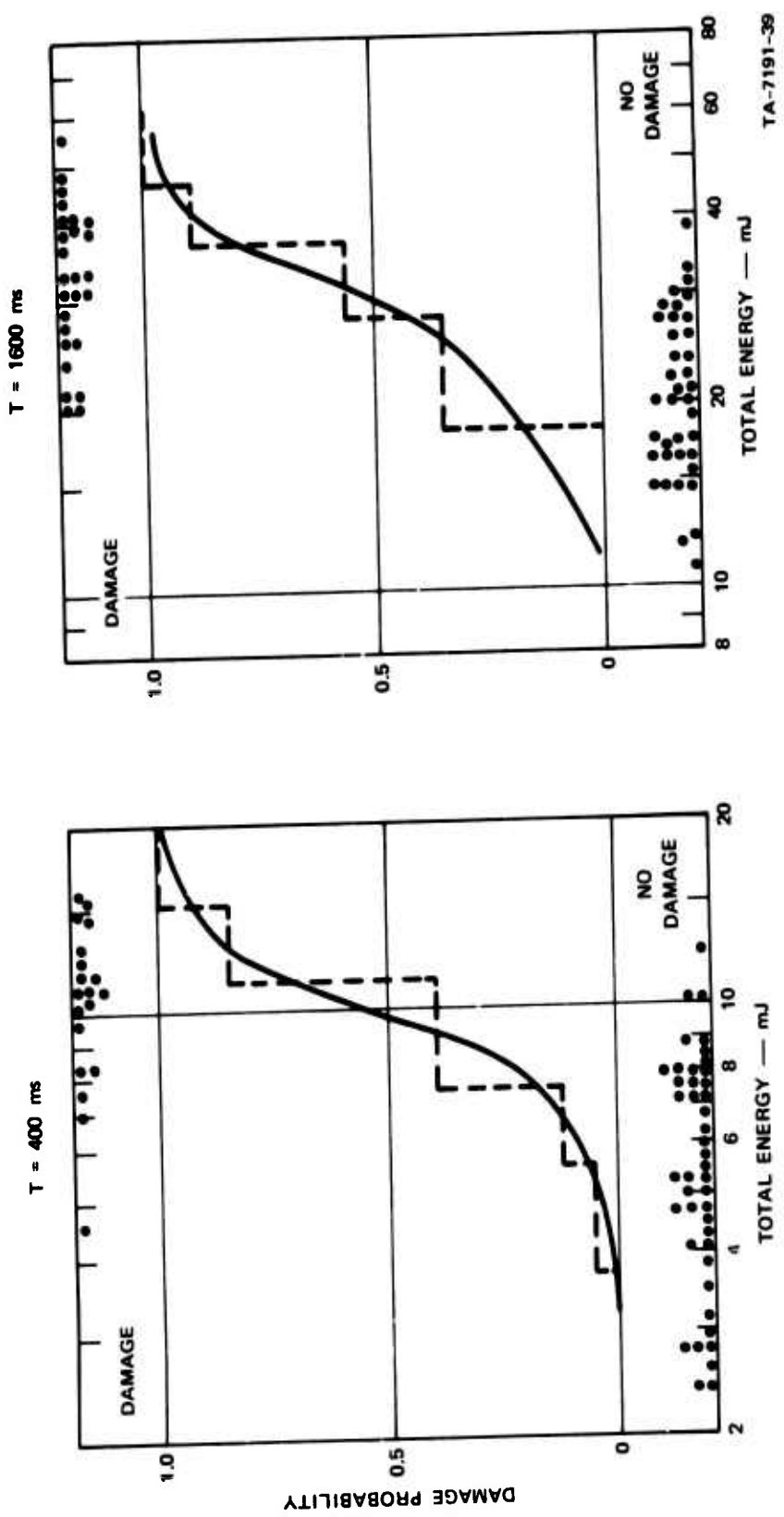
FIGURE 22   DAMAGE TO RHESUS MONKEY RETINA WITH ARGON LASER—400 AND 1600 ms, 4880 Å, 200-μ RETINAL SPOT
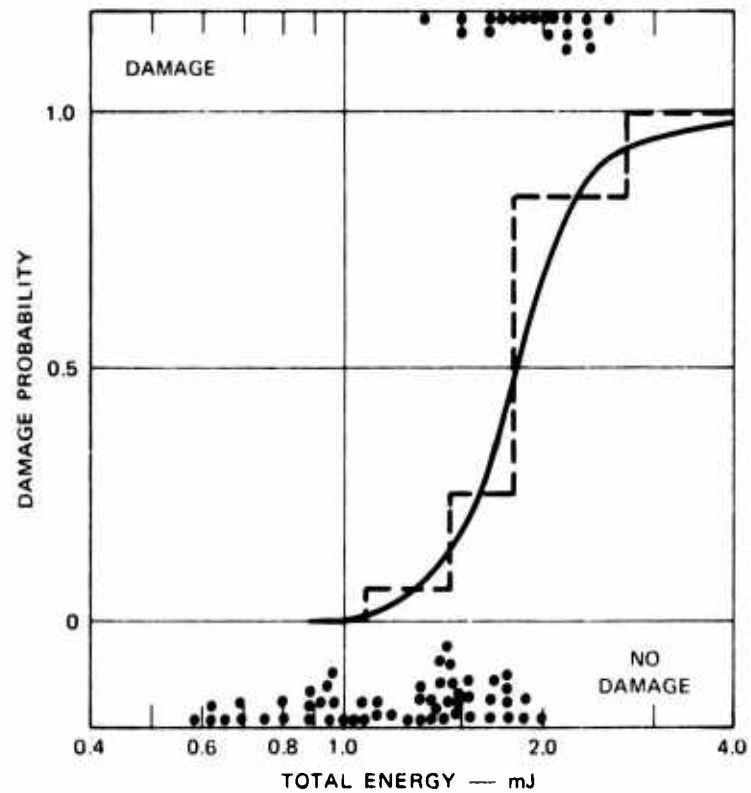
FIGURE 23   DAMAGE TO RHESUS MONKEY
             RETINA WITH ARGON LASER—
             80 ms, 4880 Å, 100-μ RETINAL
             SPOT

A plot of the argon data for all retinal spots is shown in Figure 24. Here it is interesting to observe that, for the small spot size data, power for the threshold level continues to decrease as the exposure is increased. A discussion of this trend is presented in Section V.

2.   Human Exposures

Data on two human volunteers were obtained using the 4880Å wavelength of the argon laser. An exposure time of 100 ms was used in these experiments. The data are summarized in Figure 25. One eye had a melanoma; however, exposures were made to uninvolved parts of the retina. The other was a healthy eye and it gave the lower threshold,
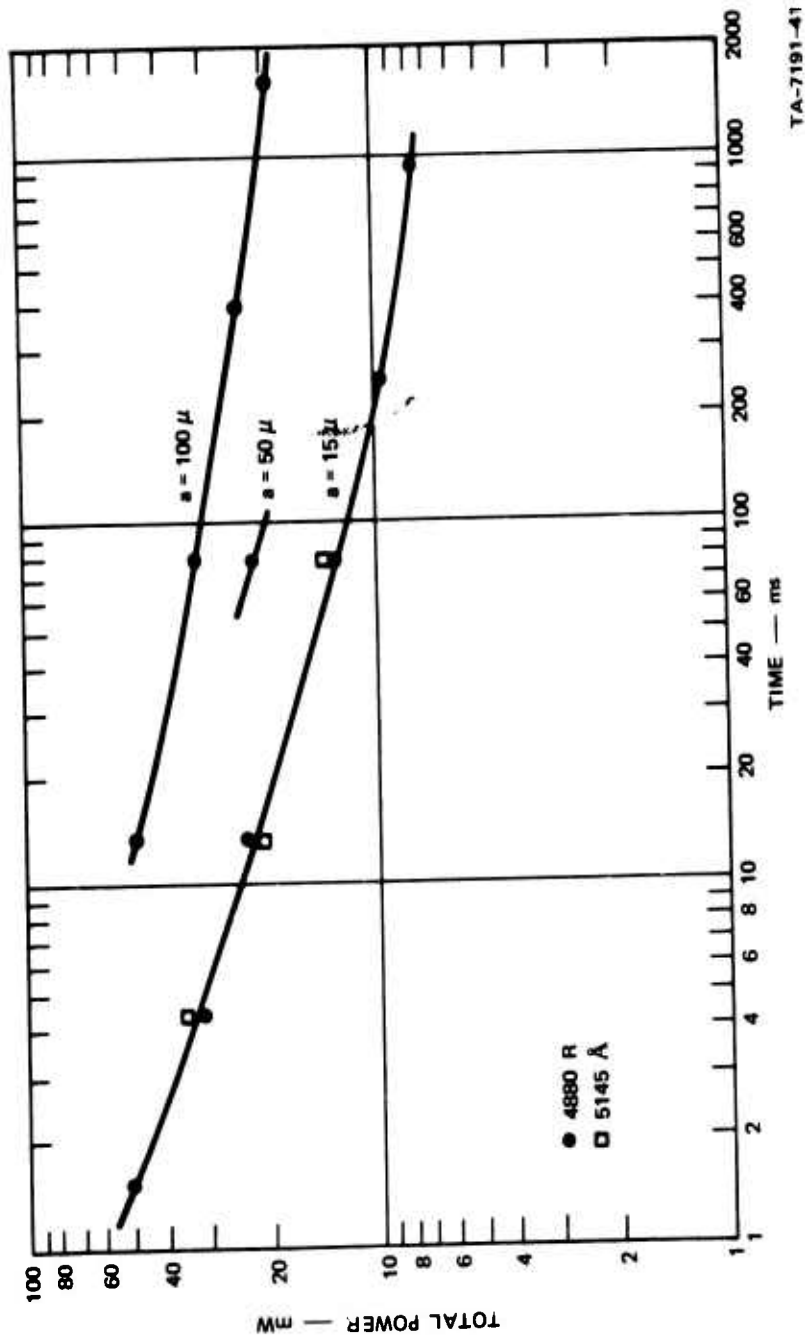
FIGURE 24   THRESHOLD RETINA DAMAGE IN RHESUS MONKEY FOR ARGON LASER.
Total power into eye to achieve 50 percent probability of damage.
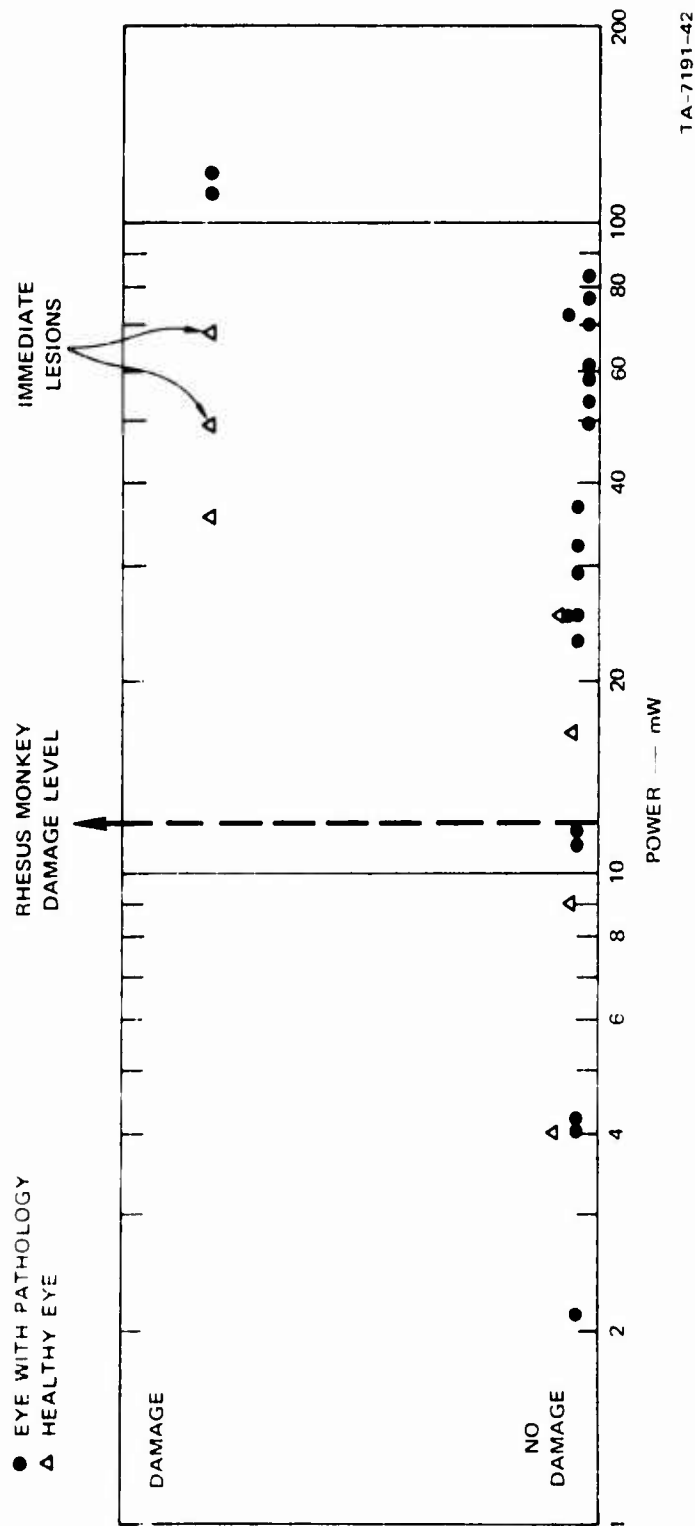
TA-7191-41

FIGURE 25   HUMAN RETINAL EXPOSURES TO ARGON LASER—100 ms, 4880 Å

1A-7191-42

probably due to its somewhat higher pigmentation and somewhat smaller retinal spot size. The estimated spot size in the healthy eye was 40μ. In comparison with the rhesus monkey data, the human data again appear higher.

C. Helium-Neon Laser Exposures

Some preliminary threshold measurements in rhesus monkeys were obtained in another program in our laboratory. The data is included here as an indication of the similarity between the argon and the Helium-Neon laser. The data are summarized in Table VII.

Table VII

HELIUM-NEON LASER DAMAGE THRESHOLD IN RHESUS MONKEYS (6328Å)

Time (ms)	No. of Eyes	Lowest Power for Observed Damage (mw)	Power for 50% Probability for Damage (mw)
13.5	4	17	23
80	4	14	18

D. Neodymium-YAG Laser Exposures

A Neodymium-YAG laser operating in a CW mode was used to obtain the threshold data in rhesus monkey eyes. The laser was always located at as large a distance from the test station as possible consistent with sufficient power to determine a threshold level. Data were first taken at about 1000 ms exposure; data were then taken at 100 and at 10 ms, where for the latter exposure the laser had to be moved closer to the test station. Finally, with the laser located at the input port of the test station, some minimal data were taken at 4.4 ms, the power into the eye being barely sufficient to obtain threshold damage. Thus, shorter exposures at this value were not attempted. In this report we present the majority of the data taken at about 10, 100, and 960 ms.

The experimental animal eyes were refracted to the nearest 0.25 diopter before each experiment. An additional 1/2 to 3/4 diopter was added to the refractive lens, depending on the judgment of the nearest

38

0.25 diopter that was made on the refraction. This was done in order to obtain a better focus of the 1.06µ (10600Å) laser beam on the retina as previously discussed. A total of 20 exposures were then made in each eye: eight above the macula, eight below the macula, and four in the macular area.

The spot size in each eye was estimated by obtaining photographs of the retinal image and then running microdensitometer traces of the image. Specially sensitized Z-1 plates were employed so that exposure could be made using the output of the laser directly. The average calculated spot size, based on the photographed image was approximately 60µ. It must be emphasized, however, that since this method depends on the scattered light from the fundus for the photography, the actual spot size of the beam could be appreciably smaller than the measured spot size. This influence of scattering will be considerably more pronounced at this wavelength than at the argon and He-Ne wavelengths.

The data for the 10-ms exposures are shown in Figure 26, where the 50 percent probability for damage is seen to be about 175 mW. Similarly, Figures 27 and 28 show the data for 100- and 960-ms exposures with 50-percent points at 96 and 56 mW respectively. In Figure 29, the 50-percent points are plotted as a function of time, and it is apparent that, as with the argon laser data, the threshold continues to decrease at the longer exposures. The Neodymium-YAG data are summarized in Table VIII.

Table VIII

NEODYMIUM-YAG LASER DAMAGE THRESHOLD IN RHESUS MONKEYS

Exposure Time (ms)	No. of Eyes	Lowest Power for Observed Damage (mw)	Power for 50% Probability for Damage (mw)
10	8	130	175
100	8	64	96
960	7	37	56
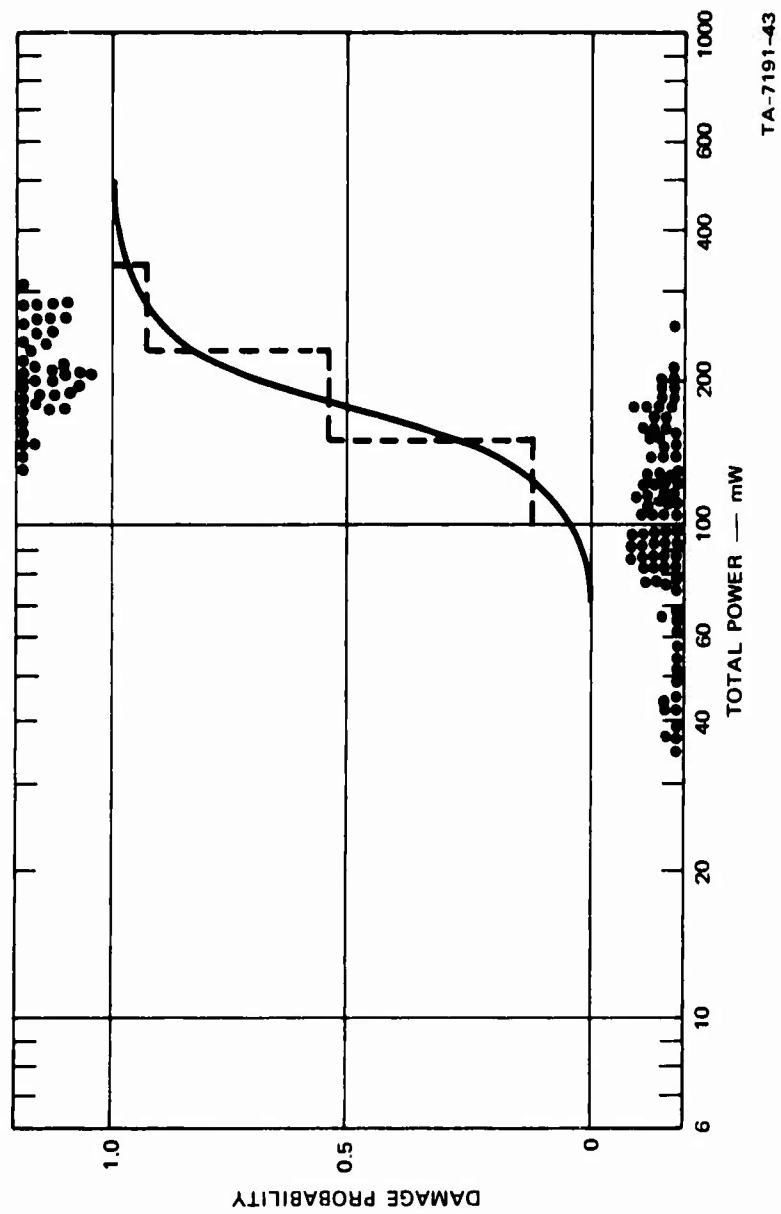
FIGURE 26   DAMAGE TO RHESUS MONKEY RETINA WITH NEODYMIUM—
YAG LASER—10 ms, 1.06 μ

TA-7191-43

40
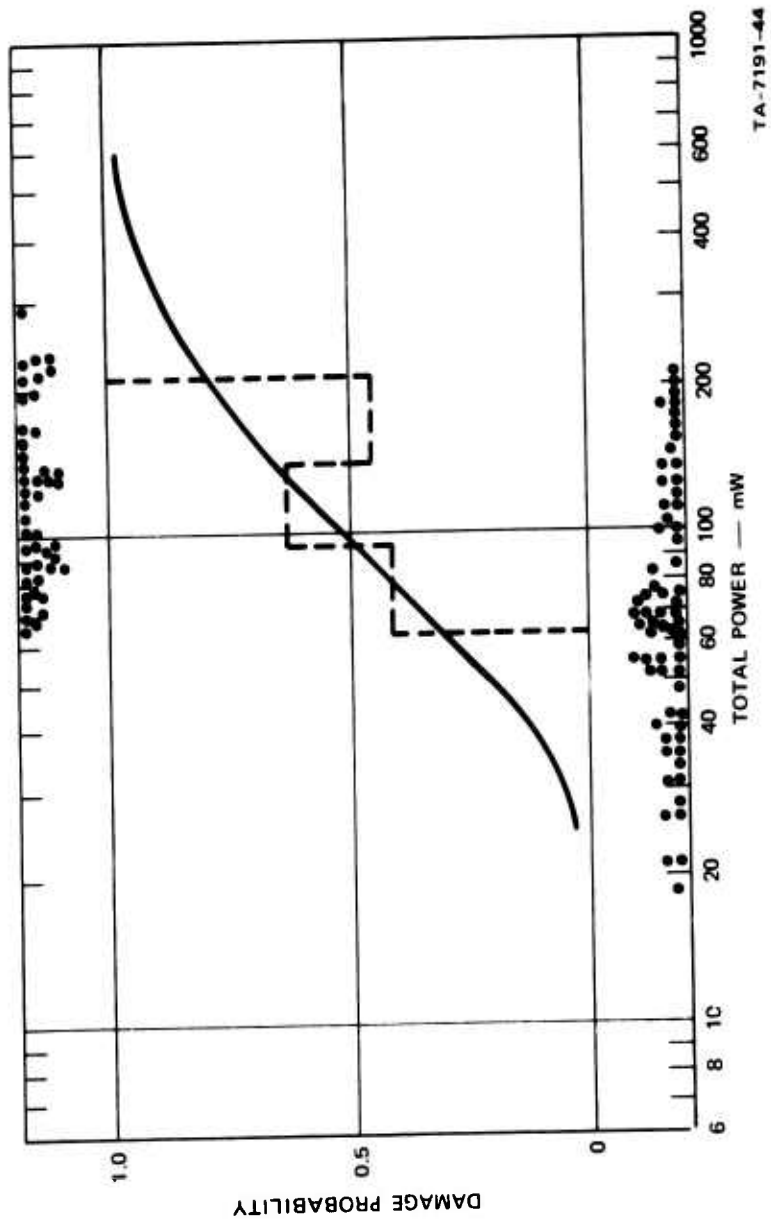
FIGURE 27   DAMAGE TO RHESUS MONKEY RETINA WITH NEODYMIUM—
YAG LASER—100 ms, 1.06 μ

41
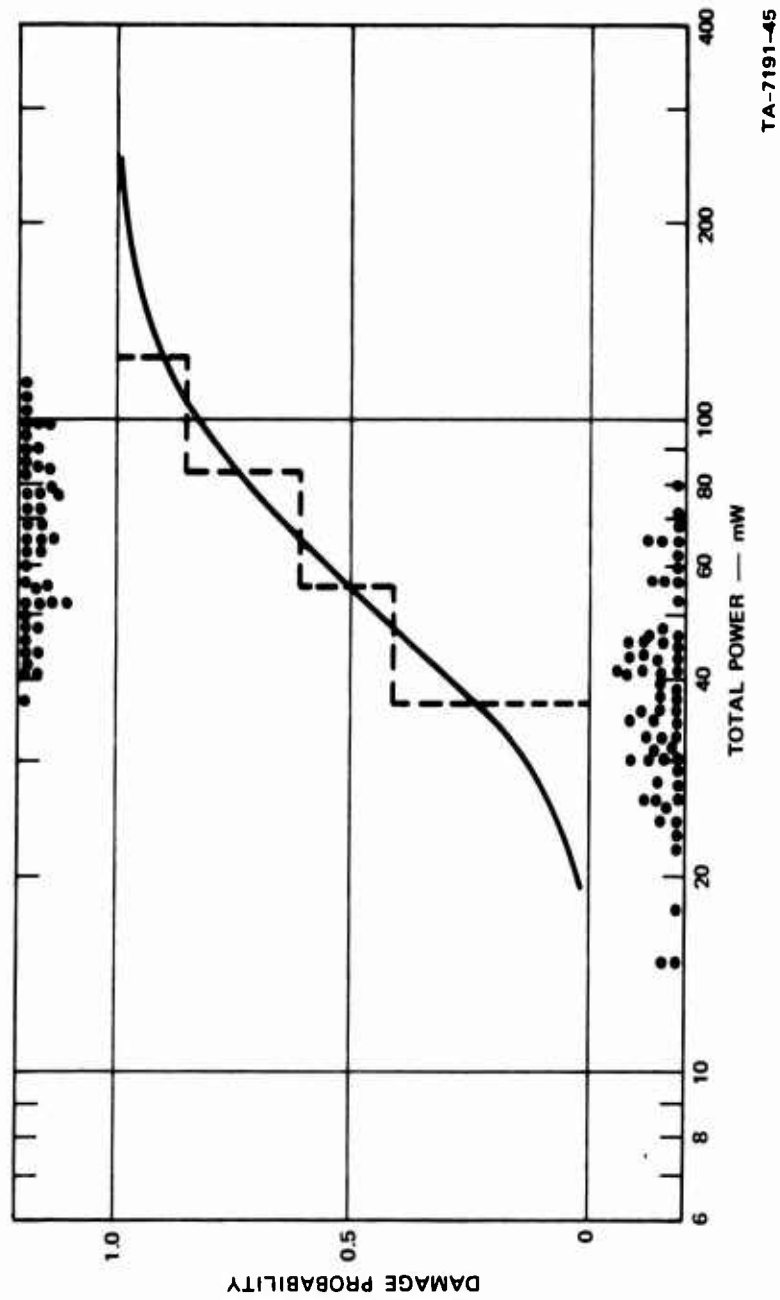
TA-7191-45

FIGURE 28   DAMAGE TO RHESUS MONKEY RETINA WITH NEODYMIUM—YAG LASER—
960 ms, 1.06 μ
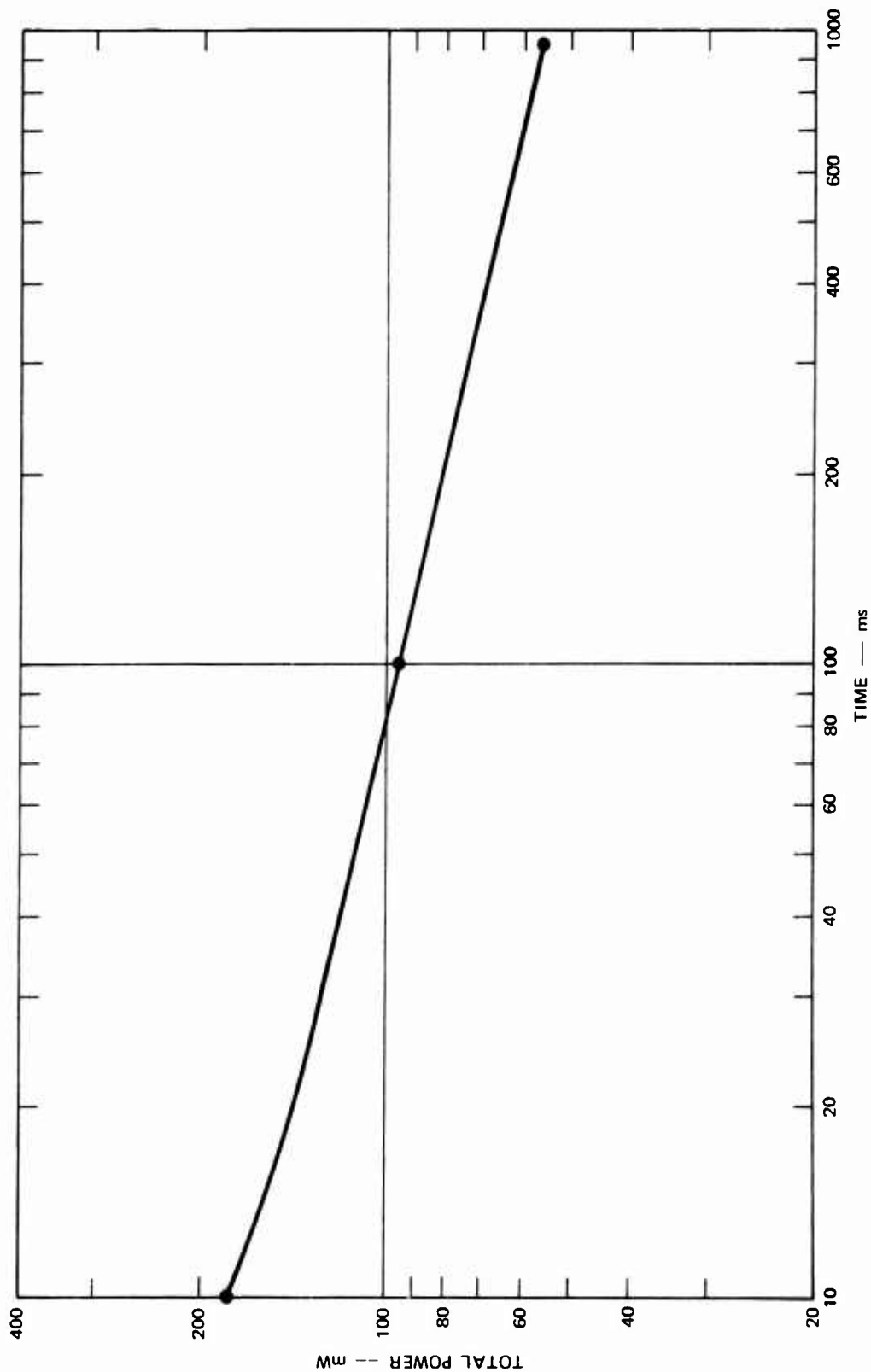
FIGURE 29   THRESHOLD RETINA DAMAGE IN RHESUS MONKEY FOR NEODYMIUM—YAG LASER
Total power into eye to achieve 50 percent probability of damage.

43

BLANK PAGE

A. Argon Laser Exposures

   1. Experimental Procedure

       Two animals were exposed with argon 4880Å laser. Four lesions were placed in each macula and the pathology of the lesions were examined at one hour and one month after exposure. The laser exposures were made at approximately three times the threshold level and two exposure times were used. Table IX summarizes the experimental protocol.

Table IX

ARGON LASER (4880Å) PATHOLOGY

Monkey	Eye	Exposure Time (ms)	Time of Enucleation after Exposure
N8	OD	10	1 hour
	OS	100	1 hour
N9	OD	10	1 month
	OS	100	1 month

       These preparations were examined by the pathologist without his knowledge of the laser energies used or the survival time of the animals after exposure. The eyes were enucleated and fixed with Newcomer's fluid in the usual way, i.e., by immediate dissection of the macular area and immediate fixation of it. The entire sample was consecutively sectioned, so that about 700 sections were prepared from each eye. The stain employed for reporting purposes of eyes N8 and N9 is the periodic acid Schiff and toluidine blue stain. This combination is intended particularly to define minimal changes associated with cytoplasmic, vascular and inflammatory components. It does not stain glia.

45

2.   N8 OD--10 ms Exposure, One Hour After Exposure

These lesions approximate 60μ in maximal diameter and are
shaped like a truncated pyramid with the small end of the base in the
pigment epithelium and the large end in the neuroepithelium. There is
pyknosis and elongation of the inner layer of visual cell nuclei with
surrounding perinuclear clearing. The outer layer of visual cell nuclei
is much less affected in this manner. Near the neuroepithelial nuclei
but in the outer plexiform layer there are a few micro blebs and bits
of displaced fragments of nuclear debris. The proximal segments of the
visual cells are often coarse and show increased basophilia. The distal
segments do not show any noticeable alterations. There is focal
bleaching of pigment epithelial cells in the line of the neuroepithelial
lesions only; micro blebs and focal thickening of Bruch's membrane is
seen. There are no inflammatory cells, no fibrin is recognized, the
nearby microcirculatory vessels in choroid and retina appear normal, and
there is no diapedesis of red cells. There is, however, a question of
pallor in the outer plexiform layer which is consistent with edema.

DIAGNOSIS--Very recent small lesions. Examples of these
lesions are shown in Figures 30 and 31.

Figure 30 (PAS/toluidine blue, 360X) shows acute lesions in
side of focal subretinal edema, lack of cellular reaction, and a small
defect in overlying outer molecular layer.

Figure 31 is a closeup of adjacent subretinal lesion, showing
pyknosis and cellular edema in visual cell layer not in true "lesion."
Displaced pigment is seen in outer segments.

3.   N8--100 ms Exposure, One Hour After Exposure

These are larger lesions than the foregoing, about 150μ in
maximal diameter, and of a more cylindrical shape. As do the previous
lesions, these have a sharp border and "punched out" appearance. Again,
there is pyknosis and elongation of nuclei in the inner layer of the
visual cells and a coarsening of the nuclear patterns of the more
outer nuclei. Perinuclear vacuolization is common in the more inner

46

FIGURE 30   PATHOLOGY PREPARATION OF ARGON LASER LESION
ONE HOUR AFTER 10-ms EXPOSURE (360X)
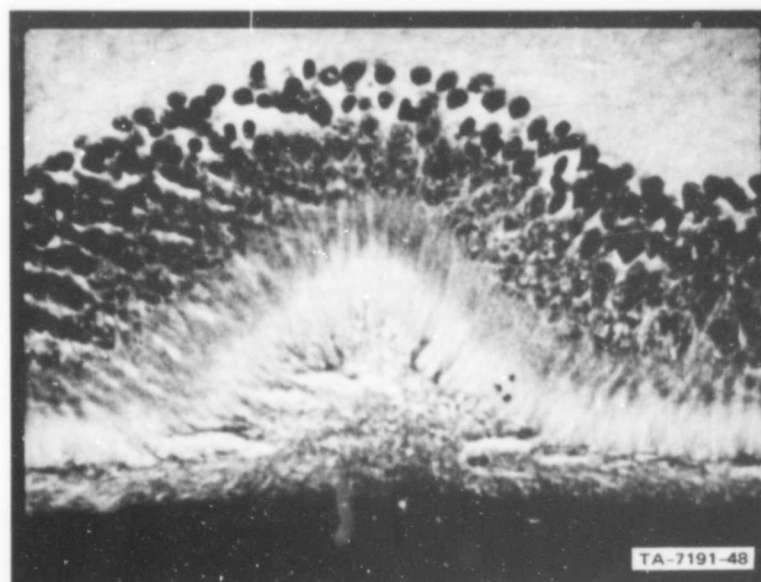
FIGURE 31   HIGH-POWER (900X) VIEW OF THE LESION
IN FIGURE 30

47

layer. No microblebs are seen. There are small numbers of periodic acid Schiff staining particles in the outer plexiform layer several lesions diameters from the disturbance in the pigment epithelia. The material does not appear to be pigment. However, there is displacement of very fine bits of pigment into the visual cell layer at the level of the segments principally, but also in the nuclear layer to a very slight degree. Where the "tails" of the visual cells dip into the pigment epithelia, there is coagulation of neuroepithelial outer segments. Bleb formation also occurs here, but not in the nuclear layer of the neu- roepithelia (as previously mentioned). The pigment cells in the line of lesion sometimes contain swollen, rounded and quite prominent pigment granules whose periodic acid Schiff staining seems to have been enhanced over normal. Although the pigment cell nuclei are darkened or their out- lines occasionally rendered indistinct, pyknosis is seen only in the layer of connective tissue nuclei immediately below them, Bruch's membrane is intact. There is no inflammation, fibrin, diapedesis or other sign of reaction.

DIAGNOSIS--A larger lesion compared to N8 OD, but with evidence of very little more tissue destruction per unit volume than before. The changes seen are not entirely the same, comparing the two lesions. However, this one also seems to be a quite recent injury at a near- threshold value.

Examples of these lesions are shown in Figures 32-35.

Figure 32 (PAS/toluidine blue, 180X) is low-power view of focal chronic lesion. There is absence of inflammatory reaction and lack of change in appearance of lesions, compared to acute (above). Pigment defect is still visibile.

Figure 33 is a closeup of the above lesion, showing displaced particles, probably including pigment. Gross, but very focal change in cytological detail, is mainly restricted to inner portion of neuro- epithelial cells. There is dilatation of adjacent blood vessels in overlying capillary bed, but no cellular exudate.
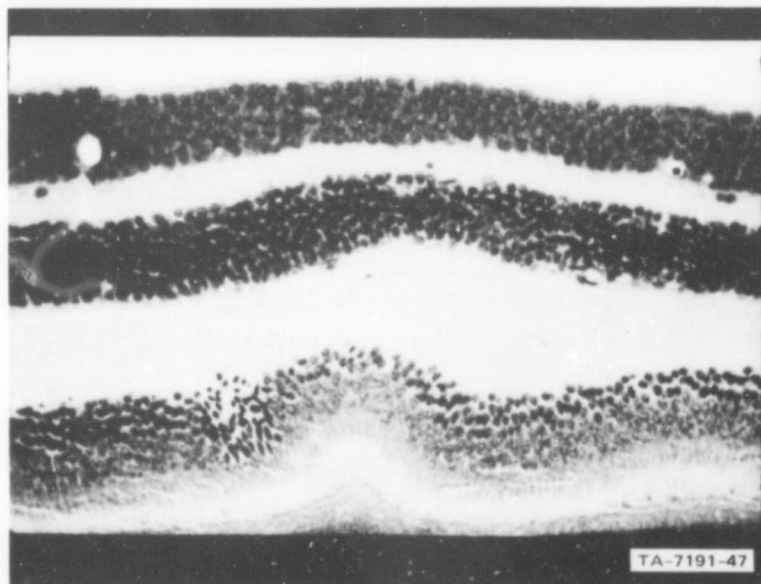
48

FIGURE 32   PATHOLOGY PREPARATION OF ARGON LASER LESION
ONE HOUR AFTER 100-ms EXPOSURE (180X)

FIGURE 33   HIGH-POWER (900X) VIEW OF THE LESION
IN FIGURE 32

FIGURE 34   PATHOLOGY PREPARATION OF ARGON LASER LESION
ONE HOUR AFTER 100-ms EXPOSURE (180X)
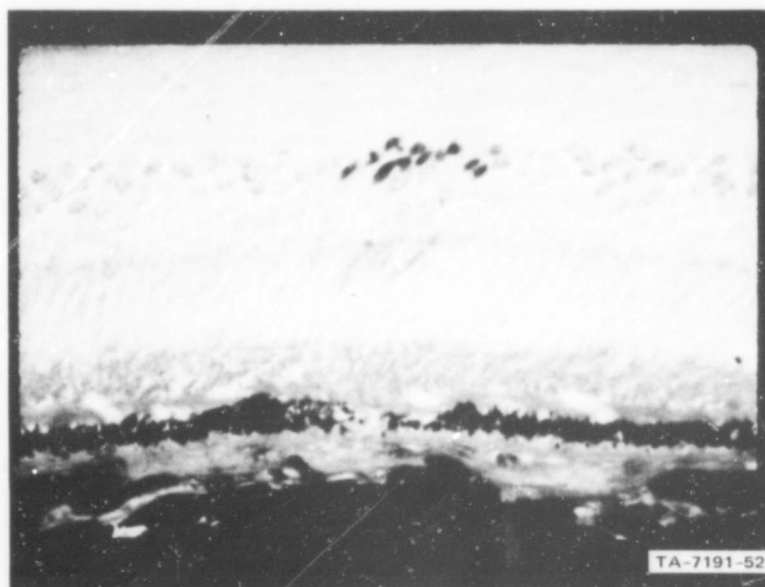
FIGURE 35   HIGH-POWER (900X) VIEW OF THE LESION
IN FIGURE 34

Figure 34 (PAS/Toluidine blue, 180X) shows another chronic focal lesion, sililar to above.

Figure 35 is a closeup of Figure 34, showing thickening of ciliary portions of neuroepithelia above focal pigment defect.

4. N9 OD--10 ms Exposure, One Month After Exposure

These very small lesions present as a pit about 50μ across. The lesion in the neuroepithelium is sharply delimited. The outer layer of visual cell nuclei is partly preserved, but the inner layer is atrophic and the cells that remain are pyknotic. There is no peri-nuclear vacuolization. Over the coarse, focally sparse inner segments, the outer limiting membrane is greatly thickened and has a peculiar orange color and ragged outline. Tiny granules of periodic acid Schiff staining material (but no pigment granules) are in the outer plexiform layer. The pigment epithelial cell nuclei are dark and crowded. Rare large cells with indistinct cytoplasm and large blunt nucleus lie parallel to the pigment epithelia and immediately upon their retinal surfaces. These are probably fibroblasts, not glia.

DIAGNOSIS--Old chronic healed lesion with focal atrophy and little reaction or regeneration; probably a low-energy lesion.

Examples of these lesions are shown in Figures 36-39.

Figure 36 (PAS/toluidine blue, 180X) shows sharply demarcated lesion with vesicular defect overlying pigment layer.

Figure 37 is a closeup at the same lesion, showing intensified and accentuated staining along the inner side of the synaptic layer with pallor on the outer side. The microcirculation is dilated in the immediate area.

Figure 38 (PAS/toluidine blue, 180X) shows a focal lesion near the fovea. The neuroepithelia is indented rather than exploded. A "tubular" lesion leads directly into the pigment layer.
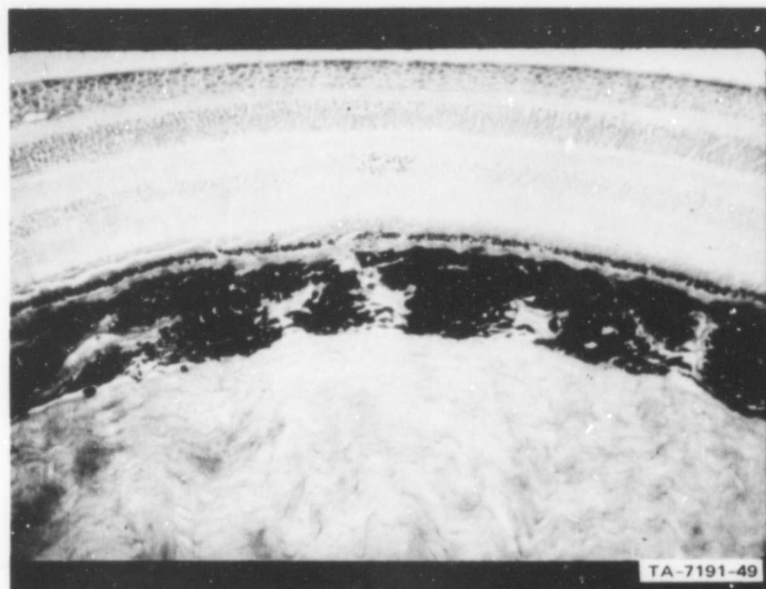
51

FIGURE 36   PATHOLOGY PREPARATION OF ARGON LASER LESION
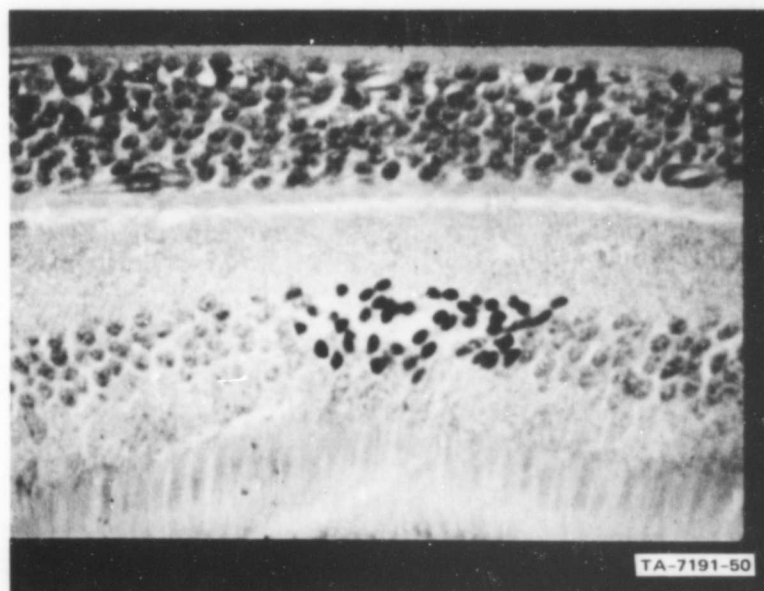ONE MONTH AFTER 10-ms EXPOSURE (180X)
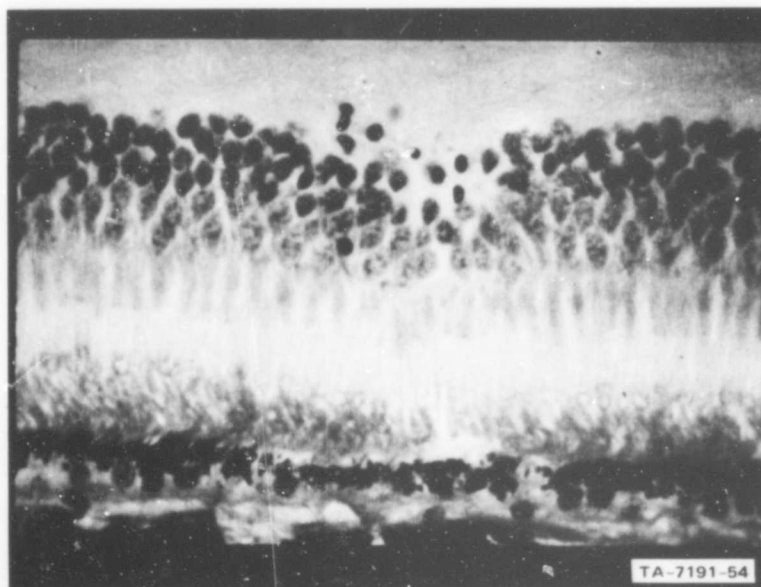
FIGURE 37   HIGH-POWER (900X) VIEW OF THE LESION
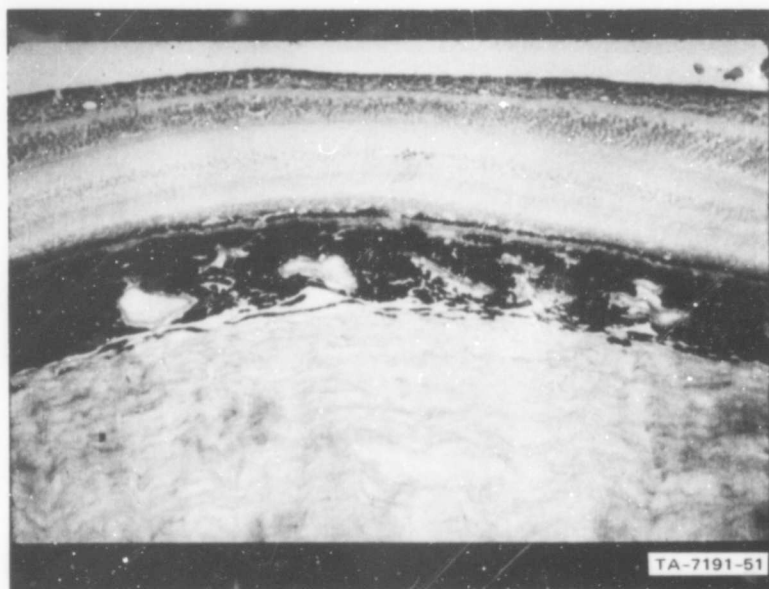IN FIGURE 36

FIGURE 38   PATHOLOGY PREPARATION OF ARGON LASER LESION
ONE MONTH AFTER 10-ms EXPOSURE (180X)
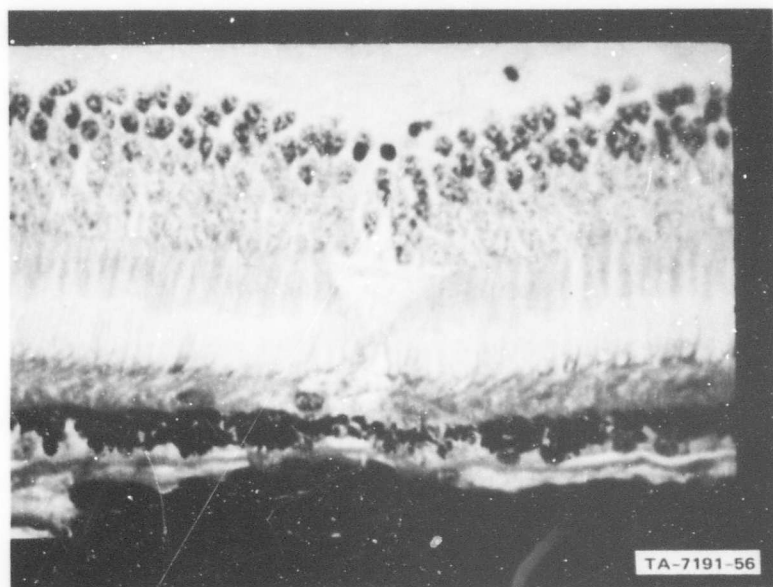
FIGURE 39   HIGH-POWER (900X) VIEW OF THE LESION
IN FIGURE 38

Figure 39--In this closeup of Figure 38, the focal defect is clearly seen associated with ragged PAS-positive swelling of the outer limiting membrane. A single infiltrative cell sits on the interlacings of pigment and neural epithelia.

5.   NO OS--100 ms Exposure, One Month After Exposure

These are large ragged lesions, between 200μ and 100μ in extent, and two of them are associated with retinal folds. It cannot be determined whether the folds are postmortem artefact, although one may have been present in life. There is a considerable atrophy of visual cells, particularly in the innermost layers, throughout the lesions. Other nuclei in these areas are pyknotic, condensed or indistinguishable from normal, i.e., there is a variegated cellular lesion. Some nuclei show elongation and displacement toward the outer limiting membrane. Some of the inner segments are condensed and basophilic. The pigment epithelim cells in the area of the lesions are crowded and their nuclei are somewhat more basophilic compared to similar features of the normal retina included in the same histological sections. In the connective tissue of the choriocapillaris immediately below Bruch's membrane are occasional neutrophiles and plasma cells.

DIAGNOSIS--There is an atrophic lesion of the visual cell layers, particularly the inner ones, and there is also a chronic reaction in the underlying choroid with evidence of continued inflammation. This is a lesion at least two weeks old, at fairly low energies.

Examples of these lesions are shown in Figures 40 and 41.

Figure 40 (PAS/toluidine blue, 180X) shows widespread pyknosis in neuroepithelia, probably due to more than one lesion. Separation is artefactual.

Figure 41 is a detail of above, showing endothelial swelling and microvascular dilatation in inner layers with emigration of damaged neuroepithelial nuclei, in outer layers.

The most interesting things about the small lesions of N8 OD and N9 OD is their sharply delimited and miniscule size. The failure
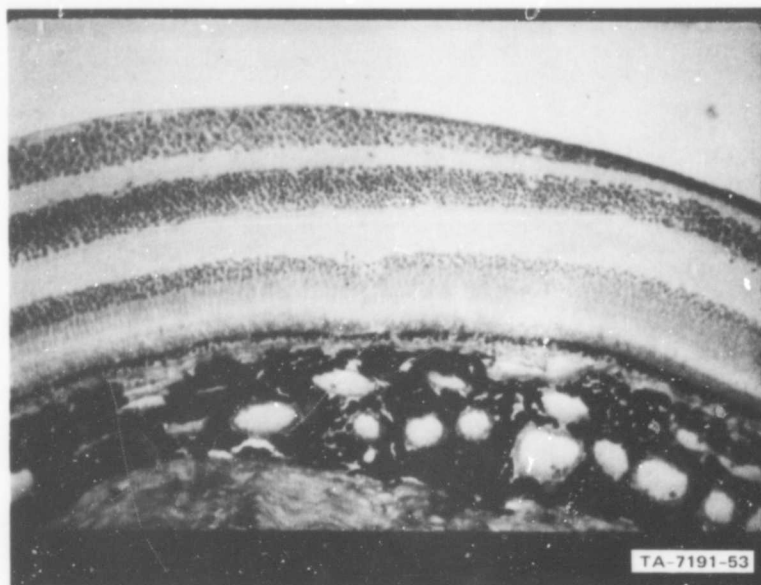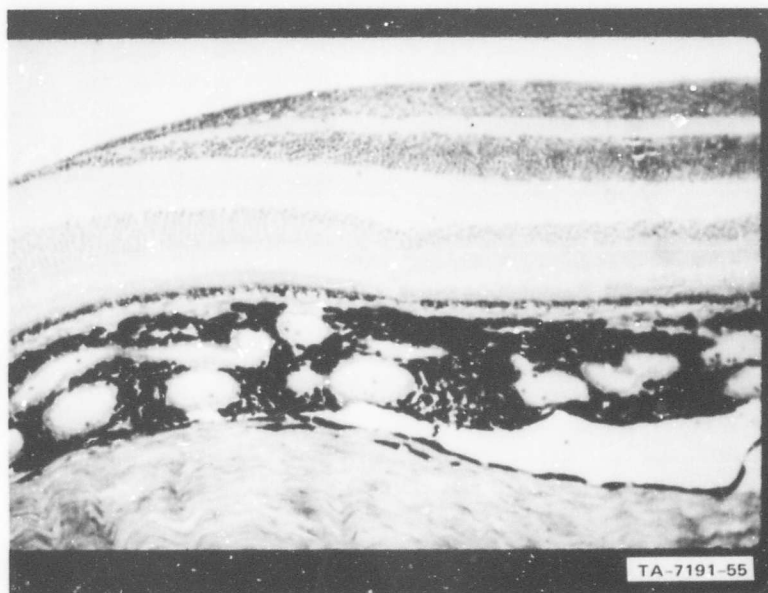
54
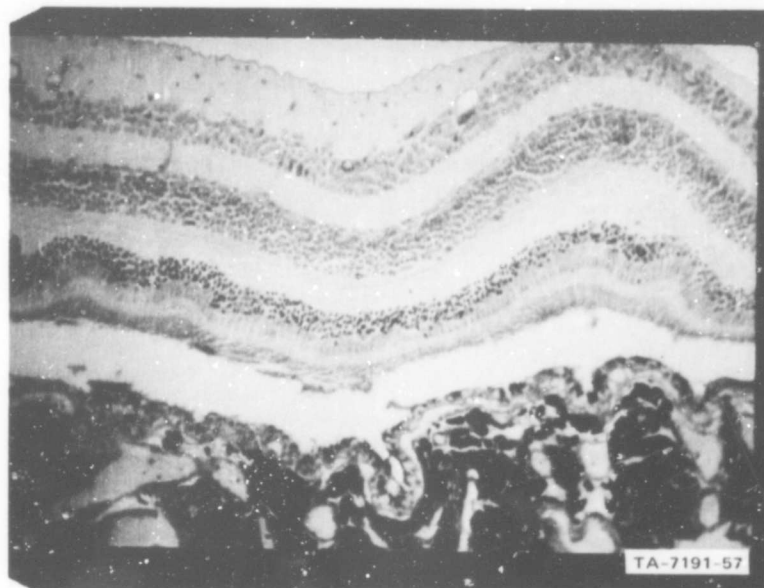
FIGURE 40   PATHOLOGY PREPARATION OF ARGON LASER LESION
ONE MONTH AFTER 100-ms EXPOSURE (180X)
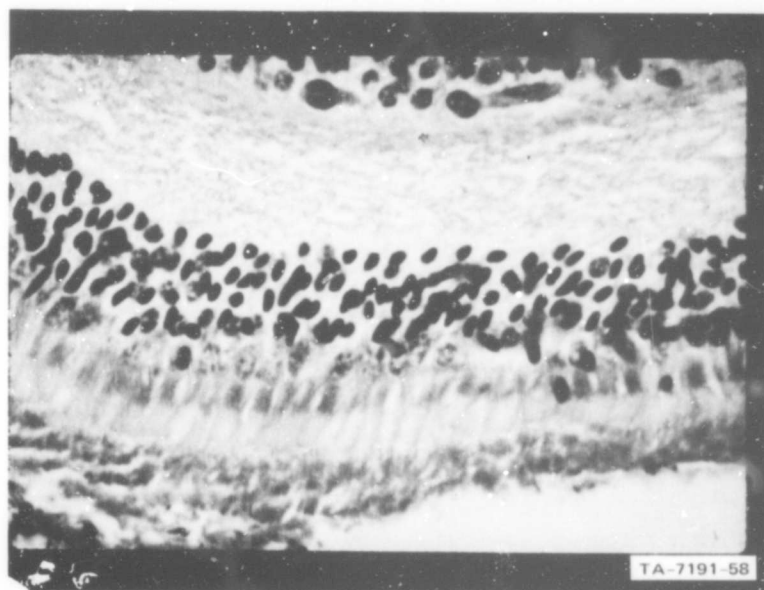
FIGURE 41   HIGH-POWER (900X) VIEW OF THE LESION
IN FIGURE 40

of the surviving nuclei to crowd around the defect and obliterate it in
N9 OD is rather surprising, and may be useful in the future study of
these lesions.

The development of a chronic inflammatory reaction in the case
of N9 OS is particularly interesting. No cause for the continued reaction
is immediately apparent. The failure of any definable gliosis or true
hyperplasia of pigment cells to develop contrasts with those features
after large lesions (with the long-pulse ruby laser).

Certain features of the morphology of the outer plexiform
layer in N8 OS and N9 OS OD, including local pallor, vascular dilatation
at the junction with the outer molecular layer, and chromatophilia of
the synapse layer, suggest that the elusive histological counterpart for
"ophthalmological edema" is at least partially represented in this layer.

B. Q-Switched Neodymium Exposures

    1. Experimental Procedure

One animal was used in this brief study of the pathology of
Q-switched neodymium laser lesions. Four lesions were placed in the
macular area of each eye at a level approximately three times threshold.
One month after laser exposures were made to the right eye, the left
eye was exposed and the animal was sacrificed one hour after the second
laser exposures.

    2. OD--One Month After Exposure

This slide is technically difficult to interpret. The macular
area has in part not been included in the block. These lesions are
typified by a thinning or atrophy of the visual cell layer without any
infiltrative or proliferative reaction. The pigment epithelium cells
in the area are rather swollen and irregular. In general, the outer
nuclei of neuroepithelia are better preserved than the inner. In some
cases, pyknotic nuclei migrate into the area of the segments. These
are probably pyknotic neuroepithelia rather than infiltrative
oligodendroglia or lymphocytes. These are moderate sized lesions which
do not show evidence of proliferative reaction in the acute or chronic

phase. The occurrence of damage during the chronic phase, at distances far removed from the original lesions, suggests that some kind of physical effect was communicated from the original site of impact at time zero. The absence of hemodiderin or erythrocytes suggests that the damage did not involve a serious hemorrhage.

3. OS--One Hour After Exposure

The immediate lesions are moderate-sized and fairly well demarcated--about 150µ in diameter. The most outstanding characteristics is the subretainal swelling in each of three lesions studied, a feature which displaces the nuclei of the neuroepithelia inward. The result is a U-shaped lesion, the arms of which sit on the damaged pigment epithelium and convexity of which pushes into the outer plexiform layer. The latter is definitely compressed, and the layer of synapses on its inmost border appears to be noticeably more demarcated than is usual.

The cellular lesion in the layer of visual cells is that of pyknosis, perinuclear edema, thickening of the outer limiting membrane, and outward migration of nuclei. There is a peculiar, stippled, basophilic degeneration of the inner segments of the cells located in the center of the lesion which alternates with a coarse blob-like prolongation of other nearby segments in an outward direction. The pigment epithelium is discontinuous, and there is necrosis of pigment cells beneath the neuroepithelial lesion. Bruch's membrane appears to be intact. There is no infiltrate or inflammatory reaction, and no proliferation.

Examples of these lesions are shown in Figures 42 and 43.

Figure 42 (Phosphotungstic acid hematoxylin, 180X) shows an excellent example of the "explosive" or expansile type of lesion. There is almost certainly subretinal edema.

Figure 43 is a detail of the above, showing the peculiar stippled segmental damage, which is highly selective among adjacent cells.

57
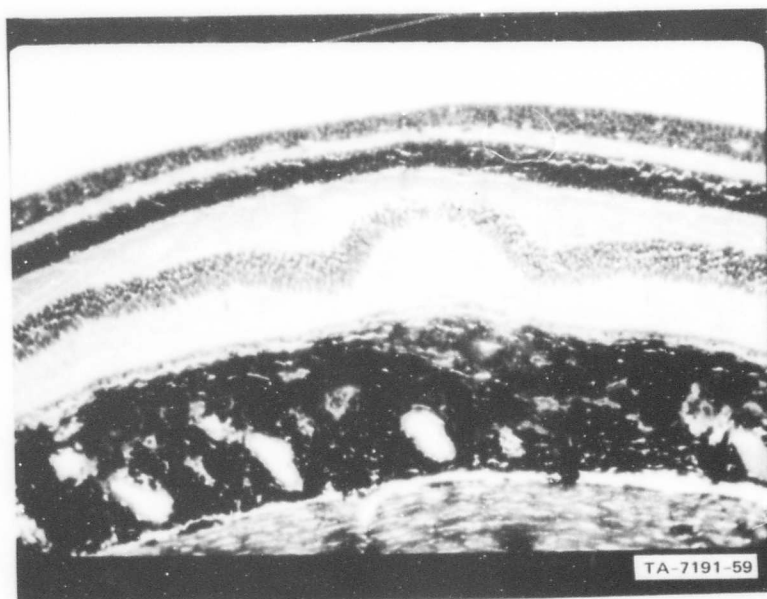
FIGURE 42   PATHOLOGY PREPARATION OF Q-SWITCHED
NEODYMIUM LASER LESION ONE HOUR
AFTER EXPOSURE (180X)
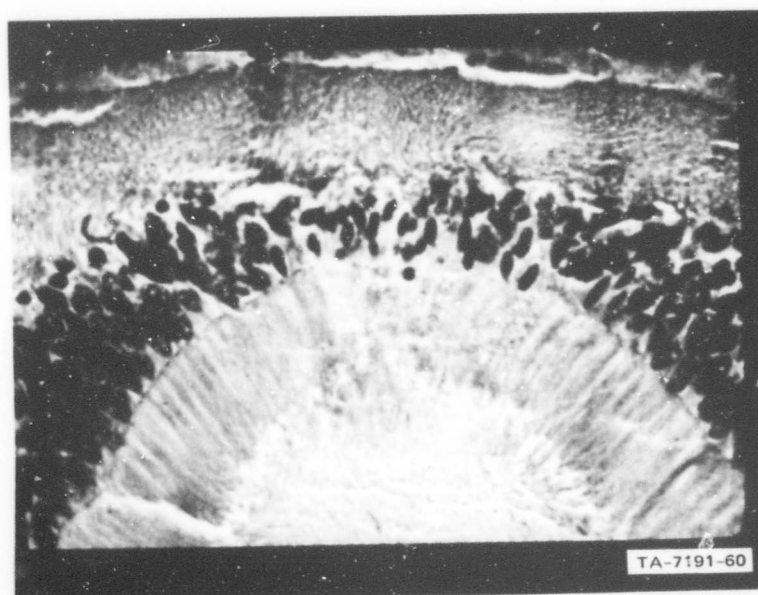
FIGURE 43   HIGH-POWER (900X) VIEW OF THE LESION
IN FIGURE 42

58

V   DISCUSSION OF LASER RETINAL DAMAGE THRESHOLDS

A.   Rhesus Monkey Laser Damage Thresholds

In this section we summarize the data reported in this report, along with some data from previous reports.[5,6]

The threshold data for small spot-sizes in rhesus monkeys were plotted in Figure 44. Although the average spot-size associated with the various lasers is slightly different, the data are plotted in the figure in terms of peak power without correction for spot size. This is done in order to make a few qualitative comments on the general trends in the data. However, as will be pointed out later, there appears to be an anomalous behaviour of threshold data which tends to make the damage less sensitive to spot-size than is expected on theoretical grounds.

The data shown in Figure 44 appear to be consistent with a thermal damage mechanism. Although there is a wide gap between the Q-switched laser data and the long-pulsed and CW laser data, the trend shows that the damage level is relatively constant with total energy in the short times where thermal relaxation during exposure can only play a negligible role. At longer times of exposure, ($\gtrsim$ 1ms) thermal conduction from the exposed areas begins to play a strong role and consequently the curves begin to level off somewhat. It is interesting to note however, that the curves continue to decrease slowly even at the longer exposures where, for small spot sizes, thermal equilibrium is usually assumed to have taken place. This effect will be briefly discussed in the next section.

The threshold data shows little difference between the 4880 and the 5145Å wavelengths of argon. The curve drawn for the ruby (6943Å) and the He-Ne (6328Å) data appears to be somewhat higher than the argon laser thresholds. This is consistent with the fact that melanin granules in the pigment epithelium and the choroid are less absorbing at these longer wavelengths.

59
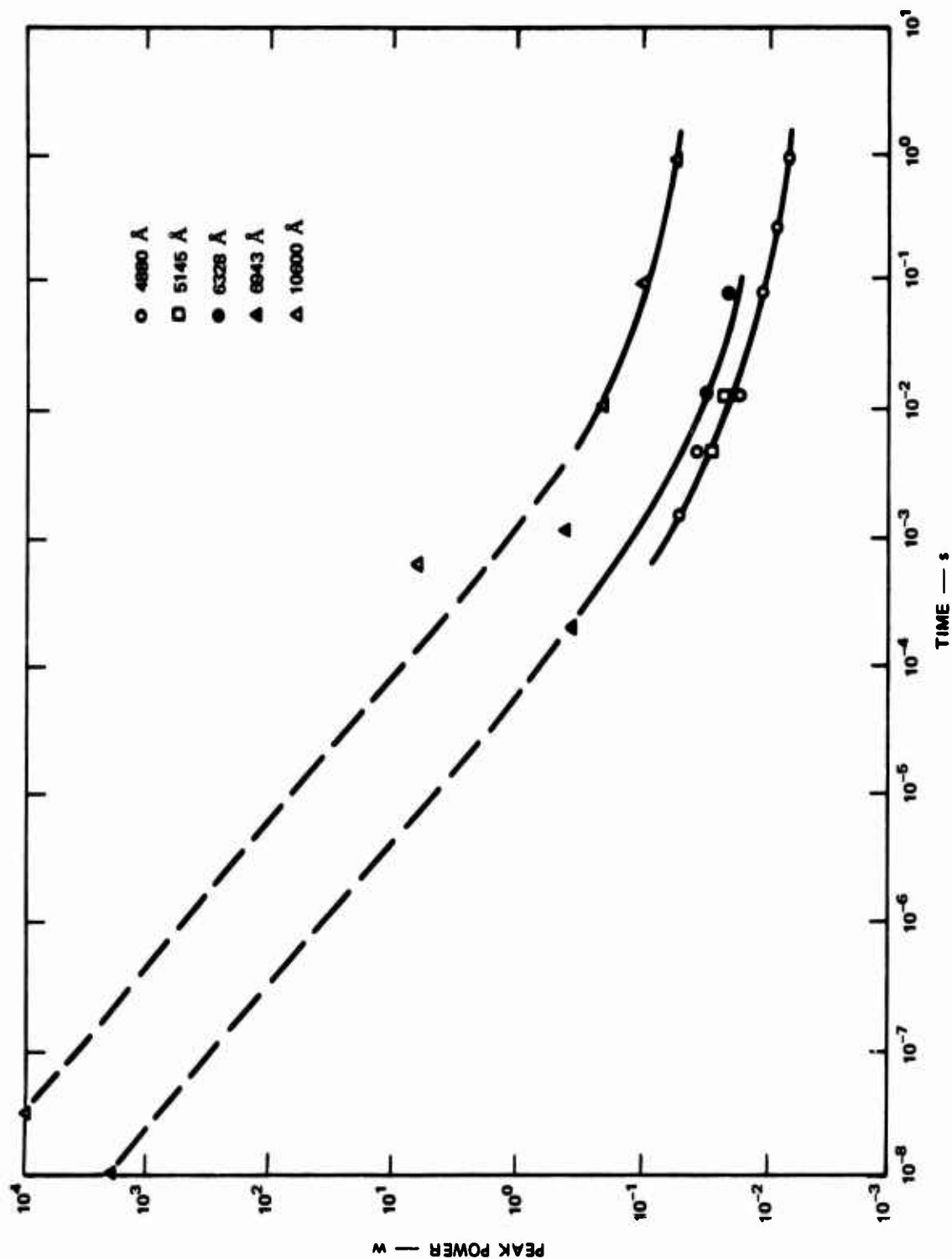
FIGURE 44   RETINA DAMAGE THRESHOLD IN RHESUS MONKEY

TA-7191-61

The data for the neodymium laser (10600Å) are appreciably higher
than the other data. This is primarily due to two effects--first the
pigment absorption is appreciably less at this wavelength and second,
the ocular media are more absorbing at this wavelength. In addition,
the estimated spot sizes of the neodymium laser exposure were higher
than for the other lasers.

B.   Thermal Damage

Since temperature is a critical parameter in the normal operation
of a living cell, an increase in temperature can lead to damaging
effects. Many theories have been proposed as to how thermal damage of
cells take place. Among the current theories are that damage is due to
alterations in the genetic mechanism, inactivation of enzymes, or
denaturation of proteins.[12]

Very little work has been done on denaturation of nucleic acids.
Indications obtained by some experiments,[13] however, are that DNA
resist temperatures of 80°C for one hour. Both protein denaturation
and enzyme inactivation take place at lower temperatures.[12,14] The heat
inactivation of enzymes is generally considered to be either a particular
case of protein denaturation or a process involving the same mechanism.
Protein molecules retain their biological meaningful activity only in their
their natural state. Thus, since all physical and chemical properties
of protein molecules may be effected by denaturation,[15] denaturation is
usually harmful and results in irreversible damage to the cell.

The denaturation of proteins and inactivation of enzymes may be
analyzed as a rate process. As is known in elementary chemistry, heat
speeds up chemical reactions. A formal description of this effect was
first given by Arrhenius in 1889. He developed an empirical equation
relating the rate of chemical process to temperature. The Arrhenius
equation may be written as

$$k' = Ae^{-\frac{E_o}{RT}} , \qquad (1)$$

where k' is the reaction rate, A is the pre-exponential factor, E_o is
the experimental activation energy, T is the absolute temperature °K,

61

and R is the gas constant. The influence of temperature on reaction rate is dominantly expressed in the exponential factor, thus although A varies slightly with temperature it is usual to assume A constant in the treatment of experimental data. Since then, rigorous theoretical basis has been given for this equation in terms of statistical mechanics.[16]

Both protein denaturation and enzyme inactivation are usually first-order reactions and increase with temperature according to the Arrhenius equation. The decisive step in the complex inactivation chain is due to a single action and thus the reaction is unimolecular and follows first-order kinetics. Thus, the concentration of the molecule has a time dependence given by:

$$\frac{dc}{dt} = k'c \quad , \tag{2}$$

where c is the concentration. The surviving fraction s may thus be expressed in the form

$$s = \frac{c}{c_o} = e^{-\int_0^t k' \, dt} \tag{3}$$

where c_o is the original concentration. This equation may be rewritten in the form

$$\ln s = \ln \frac{c}{c_o} = -A \int_0^t e^{-\frac{E_o}{R(T_o + \psi)}} \, dt, \tag{4}$$

where T_o is the ambient temperature, and ψ is the temperature rise due to thermal input beginning at $t = 0$.

The overall problem of thermal damage to biological system must therefore involve the solution of the thermal conduction equation in order to determine ψ the temperature variation with time. The temperature ψ must then be employed in Eq. (4) to solve the integral equation for a given survival ratio.

C. Retinal Damage from CW Lasers

Retinal damage caused by bright white-light sources and lasers is thermal in nature. The first attempt at a theory for retinal burns was developed by Vos.[17] Since then a number of model studies have been reported for CW and pulsed sources.[18-22] In two of these studies[21,22] effects other than thermal were shown to be negligible, even for Q-switched lasers.

In this section we consider a simple thermal model in order to discuss qualitatively the experimental observations that have been made with the CW lasers. Two characteristics will be discussed: first, the trend of the threshold level to continue to decrease as the exposure time is increased, and second, the variation of threshold with spot size.

The melamin granules in the pigment epithelium are located in the anterior part of the epithelium cells in a thickness of approximately 4μ. Thus, for a simple model we assume the absorption due to the pigment epithelium takes place uniformly in a disc-shaped region 2ℓ thick with a radius a.

The temperature rise $\psi(t)$ at the center of the absorbing layer is given by:[23]

$$\psi(t) = \frac{Q}{\rho c} \int_o^t \left(1 - e^{-\frac{a^2}{4Kt}} \right) \text{erf} \frac{\ell}{2\sqrt{Kt}} \, dt \tag{5}$$

where ρ - density, c - heat capacity, and K - diffusivity.

Using Eq. (5), the temperature rise at the center of the pigment epithelium was calculated for a number of image sizes and plotted in Figure 45. It is important to notice that although initially the temperature rise is rapid, the temperature continues to rise slowly for times much longer than the time usually interpreted as the thermal equilibrium point. If the choroid absorption was included the temperature rise from its thermal contribution would contribute even more to the continuous rise of the temperature.
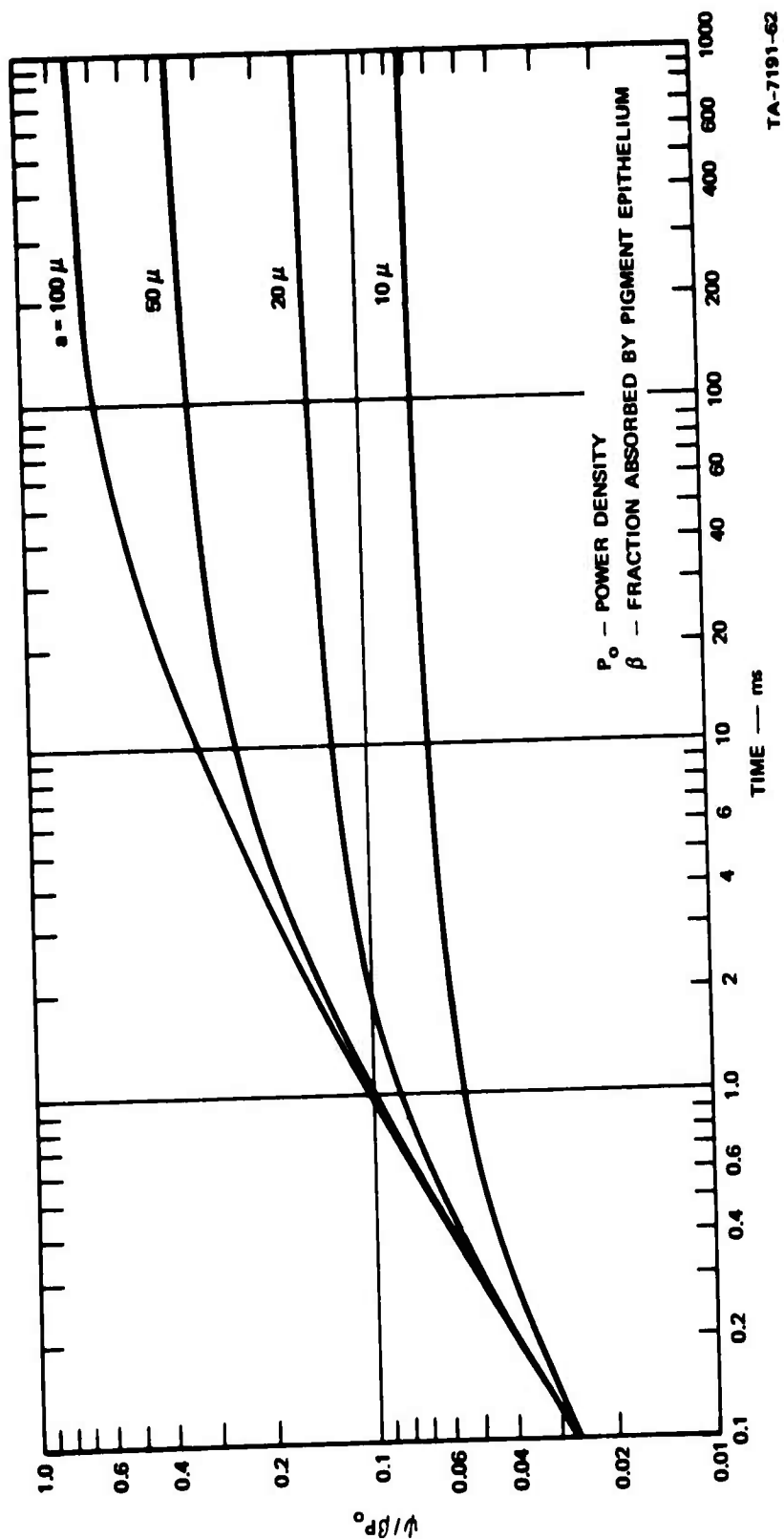
63

FIGURE 45   TEMPERATURE VARIATION AT CENTER OF ABSORBING LAYER

P_o – POWER DENSITY
β – FRACTION ABSORBED BY PIGMENT EPITHELIUM

TA-7191-62

64

We next consider a simple solution of the reaction rate process as expressed in Eq. (4) for the survival ratio. The experimental determination of threshold is a rather gross examination of the exposed site and it is unknown what the survival fraction is when damage is observed. However, since the solution of Eq. (4) is very insensitive to the survival fraction, we select arbitrarily a valve of $\frac{c}{c_o} = \frac{1}{e}$. Thus Eq. (4) becomes

$$A \int_0^t e^{-\frac{E_o}{R(T_o + \psi)}} dt = 1 \quad . \tag{6}$$

The solution of this equation with the temperature rise given by Eq. (5) would require computer calculation. For a simple discussion we assume that the temperature rise ψ is held constant for a time t. In this case Eq. (6) becomes

$$At \; e^{-\frac{E_o}{R(T_o + \psi)}} = 1 \quad . \tag{7}$$

From this equation we can obtain a relation between the ratio of two exposure times and the temperature rises associated with these exposure times. The relation can be easily brought into the form

$$\ln \frac{t_1}{t_2} = \frac{E_o}{R} \left[\frac{1}{T_o + \psi_1} - \frac{1}{T_o + \psi_2} \right] \tag{8}$$

In a steady-state situation, the temperature in the irradiated volume is proportional to the heat generating function, which in turn is proportional to the power density in the beam. Thus

$$\frac{\psi_2}{\psi_1} = \frac{P_2}{P_1} \tag{9}$$

where P is the power density in the beam. Thus, using Eq. (8), we calculate the variation of $\frac{P}{P_1}$ as a function of the time of the exposure time. We assume

$$T_o = 310^\circ K \qquad \psi_1 = 10^\circ C$$

$$50,000 < E_o < 200,000 \; cal/mole$$

65

The range of activation energy selected is that associated with the denaturation of proteins and the inactivation of enzymes.[12] The calculated curves are shown in Figure 46. Thus, under conditions where the temperature is very quickly brought to a certain level and maintained there for a time t, the threshold of damage (associated with a fixed survival ratio) will follow a curve that falls somewhere between the two curves. It is apparent that there is no unique critical temperature but that the damaging temperature varies as a function of the time of the exposure. This factor coupled with the observation that the temperature is slowly rising as a function of time even for the longer retinal exposures combine to give the decreasing threshold for damage as a function of time observed for the longer exposures of the CW lasers.

We turn now to a brief consideration of variation of threshold as a function of spot size. From Figure 45 we obtain the expected variation of threshold power level for the various spot sizes at 80 ms assuming that the same temperature is reached. The relative power level is plotted in Figure 47. From the argon laser data (Figure 24), we obtain the ratio of power levels for the various spot sizes at 80 ms. These are also plotted in Figure 47 with the normalization arbitrarily made at the 200μ spot size. It is apparent that the experimental data do not agree with the theoretical calculations of the simple model. This anomaly is similar to the observations made with Q-switched lasers discussed previously in Section II, and is possibly due to a scattering effect of the ocular refracting surfaces and media.

D. Human Exposures

The experimental data on human volunteers, although very limited, give evidence that the lightly pigmented Caucasian human fundus is less sensitive to damage than the rhesus monkey fundus. This observation was made for neodymium, ruby, and argon lasers. The difference is partly explained by the great difference in pigmentation of the fundus. Another consideration is that the human volunteers were mature individuals while the rhesus monkeys were very young--two to three years old. Finally, the lighter fundus of the human volunteers provides less contrast for

66
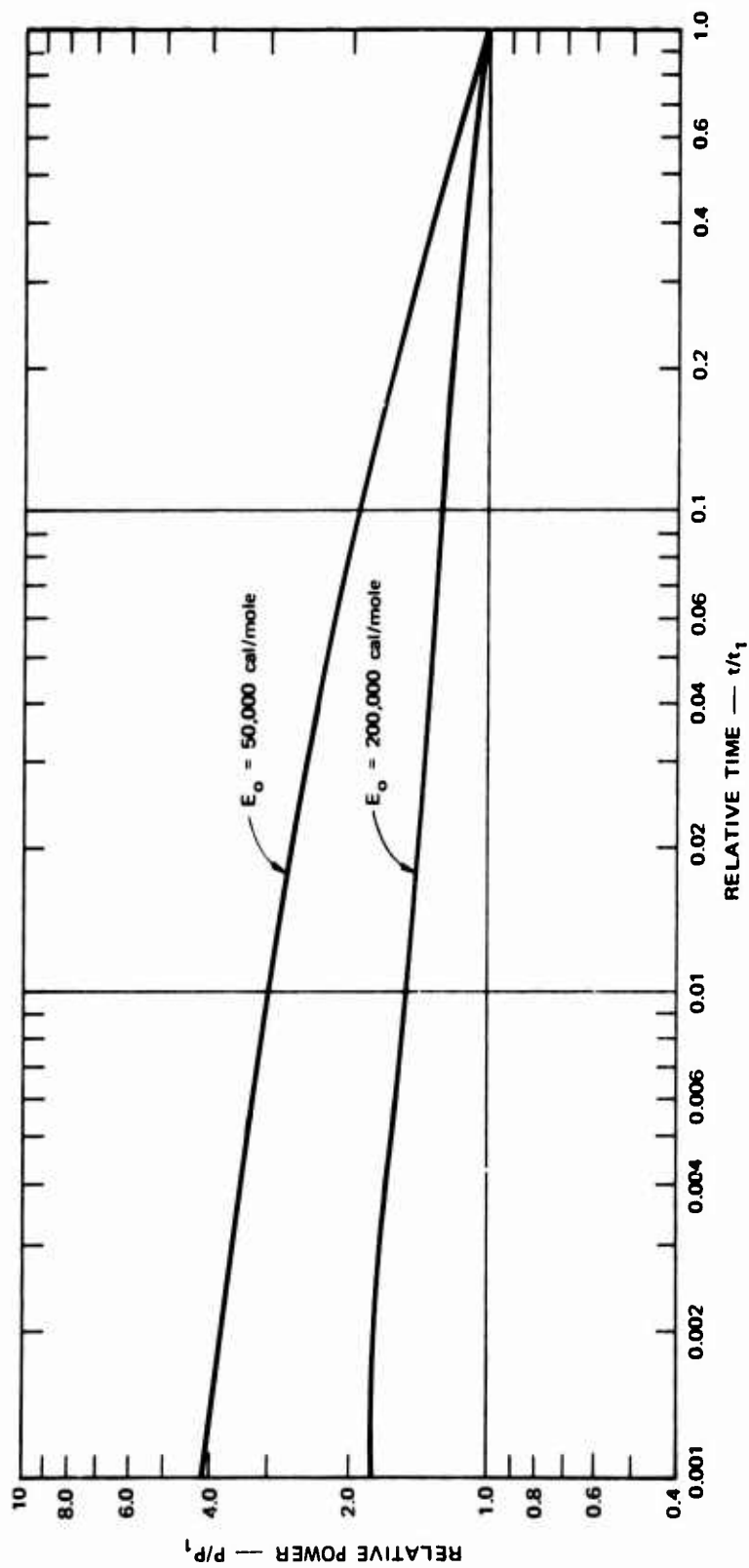
FIGURE 46   THERMAL DAMAGE BASED ON PROTEIN DENATURATION OR ENZYME INACTIVATION

TA-7191-63

67
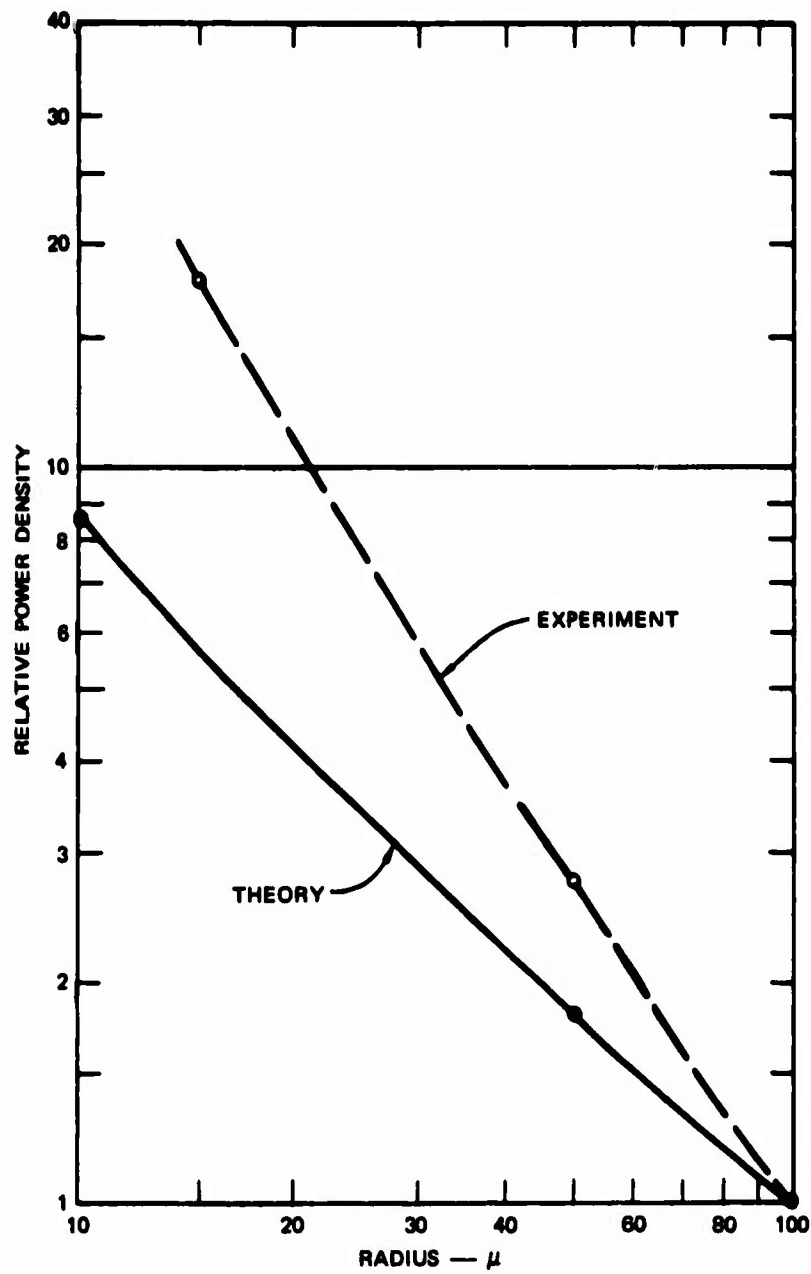
FIGURE 47   VARIATION OF POWER DENSITY
AS A FUNCTION OF RADIUS
Normalized at a = 100 μ.

the observation of small lesions in the retina. In this regard, however,
it is reiterated that all human exposures were very carefully examined
under the high magnification provided by the slit-lamp while the rhesus
monkey exposures were examined with a fundus camera and an
ophthalmoscope.

VI CONCLUSIONS

Threshold levels for retinal damage were reported for rhesus monkeys using a Q-switched neodymium laser. Data were taken in the macular and paramacular area. The macula was found to be approximately two times more sensitive than the paramacular area. Additional threshold data were obtained under more focused conditions; however, relatively little change in threshold energy was observed.

Threshold data were reported for CW lasers. Data for argon laser were reported for exposure times from 1.5 to 1000 ms for minimal spot size. Data were also taken for larger spot sizes. Limited data for a He-Ne laser were also reported. Threshold data for a Neodymium-YAG laser were obtained for exposure times from 10 to 1000 ms.

The CW laser threshold data show that the threshold level continues to decrease as the exposure time is increased. This was explained by a simple thermal model with consideration given to thermal damage caused by protein denaturation or inactivation of enzymes. An examination of threshold level as a function of spot size showed an anomally similar to that observed for the Q-switched laser. One possible explanation is that appreciable forward angle scatter takes place in the eye. The effects are thus more pronounced at the small spot size.

Experimental threshold data were obtained in human volunteers using a Q-switched neodymium and ruby lasers, a long-pulsed ruby laser, and an argon laser. The experimental data, although limited, show evidence that the Caucasian human fundus is less sensitive to damage than the rhesus monkey fundus.

ACKNOWLEDGEMENTS

REFERENCES

1. W. J. Geeraets, W. T. Ham, Jr., R. C. Williams, H. A. Mueller, J. Burkhart, D. Guerry, III, and J. J. Vos, "Laser versus Light Coagulator: A Funduscopic and Histological Study of Chorioretinal Injury as a Function of Exposure Time," Federation Proc., Vol.24, No. 1, Part III, Supplement 14, Section II (January-February 1965).

2. W. T. Ham, Jr. et al, "Effects of Laser Radiation on the Mammalian Eye," Trans. New York Acad. Sci., Vol.28, p. 517 (February 1966).

3. M. M. Zaret, "Ocular Exposure to Q-switched Laser Irradiation," Technical Report, Contract AFAL-TR-65-279, The Zaret Foundation, Inc., Scarsdale, New York (April 1966).

4. T. Bergqvist, B. Kleman, and B. Tengroth, "Retinal Lesions Produced by Q-Switched Lasers," Acta Ophthalmologica, Vol.44 (1966).

5. A. Vassiliadis, N. A. Peppers, R. R. Peabody, R. C. Rosan, H. C. Zweng, M. Flocks, and R. C. Honey, "Investigations of Laser Damage to Ocular Tissues," Technical Report AFAL-TR-67-170, Contract AF 33(615)-3060, SRI Project 5571, Stanford Research Institute, Menlo Park, California (March 1967).

6. A. Vassiliadis, N. A. Peppers, R. C. Rosan, K. Dedrick, H. Chang, R. C. Honey, H. C. Zweng, R. R. Peabody, H. W. Rose, and M. Flocks, "Investigations of Laser Damage to Ocular Tissues," Final Report, Contract F33615-67-C-1752, SRI Project 6680, Stanford Research Institute, Menlo Park, California (March 1968).

7. W. J. Geeraets, J. Burkhart, and D. Guerry, "Enzyme Activity in Coagulated Retina," Acta Ophthalmologica, Suppl. 76, Vol.79, p. 93 (1963).

8. A. Vassiliadis, R. C. Rosan, R. R. Peabody, H. C. Zweng, and R. C. Honey, "Investigation of Retinal Damage Using a Q-switched Ruby Laser" Special Technical Report, Contract AF 33(615)-3060, SRI Project 5571, Stanford Research Institute, Menlo Park, Calif. (August 1966).

9. Personal communication from Dr. D. N. Farrer and Dr. W. T. Ham, Jr.

10. R. G. King and W. J. Geeraets, Acta Ophth. Vol.46, p. 617 (1968).

11. A. E. Jones, D. D. Fairchild, and P. Spyropoulos, "Laser Radiation Effects on the Morphology and Function of Ocular Tissue" Annual Report, Contract DADA-17-67-C-0019, Honeywell, Inc., St. Paul, Minnesota (July 1968)

12. T. H. Wood, "Lethal Effects of High and Low Temperature on Uni-cellular Organisms", Advances in Biological and Med. Physics, Vol. IV, (1956).

13. S. Zamenhof, G. Griboff, and N. Marullo, Biochim. et Biophys. Acta, Vol. 13, p. 459 (1954).

14. F. H. Johnson, H. Eyring, and M. J. Pollisar, The Kinetic Basis of Molecular Biology (J. Wiley & Sons, New York 1954).

15. M. Joly, A Physico-Chemical Approach to the Denaturation of Proteins (Academic Press, New York 1965).

16. S. Glastone, K. J. Laidley, J. Eyring, The Theory of Rate Processes (McGraw-Hill Book Company, Inc., New York 1941).

17. J. J. Vos, "A Theory of Retinal Burns", Bull. Math. Phys., Vol. 24, p. 115 (1962).

18. W. T. Ham et al, Trans. N.Y. Acad. Sci., Vol. 28, p. 517 (1966).

19. W. P. Hansen, L. Feigen, and S. Fine, Appl. Optics, Vol. 6, p. 1973, (1967).

20. W. P. Hansen and S. Fine, Appl. Optics, Vol. 7, p. 155 (1968).

21. J. R. Hayes and M. L. Wolbarsht, Aerospace Medicine, Vol. 39, p. 474, (1968).

22. W. L. Makous, J. P. Gould, IBM Journal, p. 257 (May 1968).

23. A. Vassiliadis "Ocular Damage From Laser Radiation", to be published.

DOCUMENT CONTROL DATA - R & D

Security classification of title, body of abstract and indexing annotation must be entered when the overall report is classified)

1 ORIGINATING ACTIVITY (Corporate author)	2a. REPORT SECURITY CLASSIFICATION
Stanford Research Institute Menlo Park, California 94025	Unclassified
	2b. GROUP N/A

3 REPORT TITLE

RESEARCH ON OCULAR LASER THRESHOLDS

4 DESCRIPTIVE NOTES (Type of report and inclusive dates)
Final Report (15 March 1968 to 15 July 1969)

5 AUTHOR(S) (First name, middle initial, last name)

Arthur Vassiliadis   Robert C. Rosan, M.D   H. Cristian Zweng, M.D.

6 REPORT DATE	7a. TOTAL NO OF PAGES	7b NO OF REFS
August 1969	92	23

8a CONTRACT OR GRANT NO	9a. ORIGINATOR'S REPORT NUMBER(S)
F41609-68-C-0041	Final Report
b. PROJECT NO	SRI Project 7191
c.	9b. OTHER REPORT NO(S) (Any other numbers that may be assigned this report)
d.	

10 DISTRIBUTION STATEMENT

11 SUPPLEMENTARY NOTES	12 SPONSORING MILITARY ACTIVITY
	U.S. Air Force School of Aerospace Medicine Aerospace Medical Division Brooks AFB, Texas

13. ABSTRACT

Results of experimental investigations of threshold levels for small retinal lesions are presented. Data for rhesus monkeys include thresholds for a Q-switched neodymium laser, both in the macula and in the paramacular area. In addition, extensive data are presented for argon, helium-neon, and neodymium-YAG laser damage threshold.

Exposures of human volunteers to various lasers are reported. The lasers used were Q-switched neodymium and ruby lasers, a long-pulse ruby laser, and an argon laser.

A report on the histopathology of retinal injury in rhesus monkeys due to Q-switched neodymium and argon lasers is included.

DD FORM 1473 (PAGE 1)
S/N 0101-807-6801

14 KEY WORDS	LINK A		LINK B		LINK C	
	ROLE	WT	ROLE	WT	ROLE	WT
Lasers						
Retinal damage						
Eye damage						
Histological examination						
Histochemical examination						
Opthalmology						